

WAVE COMPUTATION ON THE POINCARÉ DODECAHEDRAL SPACE

AGNÈS BACHELOT-MOTET

ABSTRACT. We compute the waves propagating on a compact 3-manifold of constant positive curvature with a non trivial topology: the Poincaré dodecahedral space that is a plausible model of multi-connected universe. We transform the Cauchy problem in a mixed problem posed on a fundamental domain determined by the quaternionic calculus. We adopt a variational approach using a space of finite elements that is invariant under the action of the binary icosahedral group. The computation of the transient waves is validated with their spectral analysis by computing a lot of eigenvalues of the Laplace-Beltrami operator.

I. INTRODUCTION.

Some fundamental open questions regarding the nature of the universe concern its geometry and topology. They are the subject of many articles ([5], [12], [13], [17], [20] for example) in which models are compared with observations which are more accurate over the years. About geometry, after nine years of investigation, the data by WMAP (Wilkinson Microwave Anisotropy Probe) mission ¹ have provided strong evidence suggesting that the universe is nearly flat, with the ratio of its total matter-energy density to the critical value very close to one [23], but without fixing the sign of its curvature. The Poincaré dodecahedral space (PDS) is a plausible multi-connected universe model with positive spatial curvature. More precisely, PDS is the quotient of the unit 3-sphere S^3 by the group \mathcal{I}^* of covering isometries. The local geometry of the universe is described by a Friedmann-Lemaître metric, so PDS (denoted by \mathbf{K} in equations) is endowed with the spherical metric $ds_{\mathbf{K}}^2$ induced by $ds_{S^3}^2$. It is a three dimensional C^∞ compact manifold, without boundary. Such a manifold can conveniently be converted to a description as a fundamental domain. It will have the shape of a dodecahedron, with pairs of faces identified.

Many authors have studied PDS ([1],[3], [7], [12], [14], [15], [17], [21]). A stationary approach has been used in all these articles: the exact knowledge of the eigenvalues of the Laplace-Beltrami operator $\Delta_{\mathbf{K}}$ on PDS allows them to predict some results (for example the cosmic microwave background temperature anisotropies), and to compare with the WMAP observations.

In this paper we adopt the time approach previously developed in [2], where we studied a toy model of hyperbolic universe. Among several advantages, this method could be extended to investigate numerically the non-linear dynamics. The construction of PDS is detailed in the next section. In the third part we get a practical description of the particular fundamental domain \mathcal{F} that contains $(1, 0, 0, 0)$ of \mathbb{R}^4 , and also we get a numerical description of the projection \mathcal{F}_v of \mathcal{F} in \mathbb{R}^3 . We mainly use the quaternionic calculus. Next we consider the scalar wave operator $\partial_t^2 - \Delta_{\mathbf{K}}$ on the dodecahedral universe $\mathbb{R}_t \times \mathbf{K}$. Then, we compute the solutions of the wave equation in the time domain, by using a variational method and a discretization with finite elements. The domain of calculus is \mathcal{F}_v , therefore the initial Cauchy problem on the manifold without boundary \mathbf{K} , becomes a mixed problem on \mathcal{F}_v with suitable periodic boundary conditions on $\partial\mathcal{F}_v$. These boundary constraints are implemented in the choice of the basis of finite elements. We validate our results by performing a Fourier analysis of the transient waves that allows to find a lot of eigenvalues of the Laplace-Beltrami operator $\Delta_{\mathbf{K}}$ on PDS.

¹ <http://map.gsfc.nasa.gov>

II. THE POINCARÉ DODECAHEDRAL SPACE.

To be able to perform computations on PDS we need to describe it accurately. This section recalls the properties of \mathcal{S}^3 , \mathcal{I}^* and $\mathcal{S}^3/\mathcal{I}^*$ that we need to know. The 3-sphere is the submanifold of four-dimensional Euclidean space such that $x_0^2 + x_1^2 + x_2^2 + x_3^2 = 1$. The comoving spatial distance d between any two points x and y on \mathcal{S}^3 is given by:

$$d(x, y) = \arccos[x^i y_i]$$

We also use the parametrisation:

$$\begin{aligned} x_0 &= \cos \chi \\ x_1 &= \sin \chi \sin \theta \sin \varphi \\ x_2 &= \sin \chi \sin \theta \cos \varphi \\ x_3 &= \sin \chi \cos \theta \end{aligned}$$

with $0 \leq \chi \leq \pi$, $0 \leq \theta \leq \pi$ and $0 \leq \varphi \leq 2\pi$. These parametrisation leads to a convenient way to visualize \mathcal{S}^3 : two balls in \mathbb{R}^3 glued together by their boundary. The θ and φ coordinates are the standard ones for \mathcal{S}^2 . For the first ball χ runs from 0 at the center through $\frac{\pi}{2}$ at the surface. For the second ball χ runs from $\frac{\pi}{2}$ at the surface through π at the center. We use a projection p of \mathcal{S}^3 in \mathbb{R}^3 :

$$\begin{aligned} p : \quad \mathcal{S}^3 &\rightarrow \mathbb{R}^3 \\ (x_0, x_1, x_2, x_3) &\mapsto (x_1, x_2, x_3) \end{aligned}$$

That is to say, to represent a point of coordinates $(x_i)_{\{i=0,1,\dots,3\}}$ of \mathcal{S}^3 , we consider only the coordinates $(x_i)_{\{i=1,\dots,3\}}$ and discard x_0 . The two points of coordinates (x_0, x_1, x_2, x_3) and $(-x_0, x_1, x_2, x_3)$ have the same coordinates (x_1, x_2, x_3) ; they are represented by the same point. In the sequel, for any $A \subset \mathcal{S}^3$, we use A_v to denote the visualization in \mathbb{R}^3 of A , that is $A_v := p(A)$.

To define a discrete fixed-point free subgroup $\Gamma \subset SO(4)$ of isometries of \mathcal{S}^3 , one makes use of the fact that the unit 3-sphere \mathcal{S}^3 is identified with the multiplicative group \mathbb{H}_1 of unit quaternions by

$$x = (x_0, x_1, x_2, x_3) \iff q = x_0 \mathbf{1} + x_1 \mathbf{i} + x_2 \mathbf{j} + x_3 \mathbf{k}.$$

The four basic quaternions $\{\mathbf{1}, \mathbf{i}, \mathbf{j}, \mathbf{k}\}$ of the set \mathbb{H} of all quaternions, satisfy the multiplication rules $\mathbf{i}^2 = \mathbf{j}^2 = \mathbf{k}^2 = -1$, and $\mathbf{k} = \mathbf{i}\mathbf{j} = -\mathbf{j}\mathbf{i}$. They commute with every real number. The norm of q is defined by $\|q\| := x_0^2 + x_1^2 + x_2^2 + x_3^2$. The conjugate \bar{q} of $q = a\mathbf{1} + b\mathbf{i} + c\mathbf{j} + d\mathbf{k}$ is defined by $\bar{q} := a\mathbf{1} - b\mathbf{i} - c\mathbf{j} - d\mathbf{k}$.

In this paper, we are interested in the subgroup \mathcal{I}^* of $SO(4)$ called the binary icosahedral group ([19], [22], [16], [7]). It is a two sheeted covering of the icosahedral group $\mathcal{I} \subset SO(3)$ consisting of all orientation-preserving symmetries of a regular icosahedron. Indeed, for any q in the multiplicative group of unit quaternions \mathbb{H}_1 we consider $p_q : \mathbb{H} \rightarrow \mathbb{H}$ defined by $p_q(q') := qq'q^{-1}$. It fixes the identity quaternion $\mathbf{1}$, so in effect its action is confined to the equatorial 2-sphere spanned by the remaining basis quaternions $(\mathbf{i}, \mathbf{j}, \mathbf{k})$. Thus, by viewing \mathbb{R}^3 as the space of pure imaginary quaternions, subspace of \mathbb{H} with basis $\{\mathbf{i}, \mathbf{j}, \mathbf{k}\}$, we get a rotation in \mathbb{R}^3 . So p_q belongs to $SO(3)$. The map $\pi : \mathbb{H}_1 \rightarrow SO(3)$ defined by $\pi(q)(q') = qq'q^{-1}$ is a homomorphism of \mathbb{H} onto $SO(3)$. π is a two to one homomorphism as $\pi(q) = \pi(-q)$. By definition we have $\mathcal{I}^* := \pi^{-1}(\mathcal{I})$. The order of \mathcal{I} is 60, so the order of $\mathcal{I}^* = \pi^{-1}(\mathcal{I})$ is 120. \mathcal{I}^* contains only right-handed Clifford translations γ , in other words γ acts on an arbitrary unit quaternion $q \in \mathcal{S}^3$ by left multiplication and translates all points $q_1, q_2 \in \mathcal{S}^3$ by the same distance χ , i.e. $d(q_1, \gamma q_1) = d(q_2, \gamma q_2) = \chi$. The right-handed Clifford translations act as right-handed cork screw fixed-point free rotations of \mathcal{S}^3 .

Let take $\gamma = a\mathbf{1} + b\mathbf{i} + c\mathbf{j} + d\mathbf{k}$ an element of \mathcal{I}^* (with $\arccos a = \chi$), and $q = x_0\mathbf{1} + x_1\mathbf{i} + x_2\mathbf{j} + x_3\mathbf{k}$

in \mathcal{S}^3 . We can express γ as a matrix and we have:

$$\gamma q = \begin{pmatrix} a & -b & -c & -d \\ b & a & -d & c \\ c & d & a & -b \\ d & -c & b & a \end{pmatrix} \begin{pmatrix} x_0 \\ x_1 \\ x_2 \\ x_3 \end{pmatrix}$$

\mathcal{I}^* is generated by two isometries s and γ . Denoting by $\sigma = (1 + \sqrt{5})/2$ the golden number we have:

$$\begin{aligned} \mathcal{I}^* &= \langle s, \gamma \mid (s\gamma)^2 = s^3 = \gamma^5 \rangle \\ &= \left\{ \pm \mathbf{1}, \pm \mathbf{i}, \pm \mathbf{j}, \pm \mathbf{k}, \frac{1}{2}(\pm \mathbf{1} \pm \mathbf{i} \pm \mathbf{j} \pm \mathbf{k}), \frac{1}{2}(0\mathbf{1} \pm \mathbf{i} \pm \frac{1}{\sigma}\mathbf{j} \pm \sigma\mathbf{k}) \text{ (with even permutations)} \right\}. \end{aligned}$$

We see that every element of \mathcal{I}^* is a right-handed Clifford translation with χ equal to 0, π , $\frac{\pi}{2}$, $\frac{\pi}{3}$, $\frac{2\pi}{3}$, $\frac{\pi}{5}$, $\frac{2\pi}{5}$, $\frac{3\pi}{5}$, or $\frac{4\pi}{5}$. We deduce that $\frac{\pi}{5}$ is the smallest non-zero translation distance. For example \mathcal{I}^* is generated by $s = \frac{1}{2}(\mathbf{1} + \mathbf{i} + \mathbf{j} + \mathbf{k})$ and $\gamma = \frac{\sigma}{2}\mathbf{1} + \frac{1}{2\sigma}\mathbf{j} - \frac{1}{2}\mathbf{k}$. s is a right-handed Clifford translation with χ equal to $\frac{\pi}{3}$. Also, p_s is a rotation in \mathbb{R}^3 , its angle is $\frac{2\pi}{3}$ and its axis is directed by the vector $\frac{1}{\sqrt{3}}(1, 1, 1)$. γ is a Clifford translation with χ equal to $\frac{\pi}{5}$. Moreover p_γ is a rotation in \mathbb{R}^3 , its angle is $\frac{2\pi}{5}$ and its axis is directed by the vector $\frac{1}{\sqrt{3-\sigma}}(0, \frac{1}{\sigma}, -1)$.

We now consider $\mathcal{S}^3/\mathcal{I}^*$ the quotient of the 3-sphere \mathcal{S}^3 under the action of the discrete fixed-point free subgroup \mathcal{I}^* of isometries of \mathcal{S}^3 , with \mathcal{I}^* acting by left multiplication. This is the Poincaré dodecahedral space (PDS) ([19], [22], [16], [7]). To perform the computations of the waves on $\mathcal{S}^3/\mathcal{I}^*$, it is very useful to represent it by a fundamental domain $\mathcal{F} \subset \mathcal{S}^3$ and an equivalence relation \sim such that

$$(II.1) \quad \mathcal{S}^3/\mathcal{I}^* = \mathcal{F}/\sim.$$

\mathcal{F} is such that:

- $\mathcal{S}^3 = \bigcup_{t \in \mathcal{I}^*} t(\mathcal{F})$,
- $\forall t \in \mathcal{I}^*, \forall t' \in \mathcal{I}^*, t(\mathcal{F}) \cap t'(\mathcal{F}) = \emptyset$.

\mathcal{F} is a regular spherical dodecahedron (dual of a regular icosahedron), and \sim is obtained by identifying any pentagonal face of \mathcal{F}_v with its opposite face, after rotating by $\frac{\pi}{5}$ in the clockwise direction around the outgoing axis orthogonal to this last face. 120 such spherical dodecahedra tile the 3-sphere in the pattern of a regular 120-cell (see figure 3).

III. FUNDAMENTAL DOMAIN \mathcal{F} OF PDS, AND ITS VISUALIZATION \mathcal{F}_v .

We have chosen the unique fundamental domain that contains $(1, 0, 0, 0)$ to simplify calculations and visualization. In the following it will be denoted \mathcal{F} . In order to perform computations we need to know the coordinates of all points in \mathcal{F} , and the equations of its edges and faces. We also deduce the characteristics of $\mathcal{F}_v := p(\mathcal{F})$, which is our domain of calculus and visualization.

Proposition III.1. *The unique fundamental domain that contains $(1, 0, 0, 0)$ is the geodesic convex hull in \mathcal{S}^3 of these 20 vertices: $\frac{1}{2\sqrt{2}}(\sigma^2, \pm \frac{1}{\sigma^2}, 0, \pm 1)$, $\frac{1}{2\sqrt{2}}(\sigma^2, 0, \pm 1, \pm \frac{1}{\sigma^2})$, $\frac{1}{2\sqrt{2}}(\sigma^2, \pm \frac{1}{\sigma}, \pm \frac{1}{\sigma}, \pm \frac{1}{\sigma})$ and $\frac{1}{2\sqrt{2}}(\sigma^2, \pm 1, \pm \frac{1}{\sigma^2}, 0)$.*

Anyone of the 12 faces F_i of \mathcal{F} is a regular pentagon in \mathcal{S}^3 included in

$$\{(x_0, x, y, z) \in \mathcal{S}^3, \quad a_i x + b_i y + c_i z = \frac{x_0}{\sigma^2}\},$$

with (a_i, b_i, c_i) equal to $(\pm \frac{1}{\sigma}, \pm 1, 0)$, up to an even permutation.

The set of all barycenters in \mathbb{R}^4 of the vertices of F_i , denoted by F_i^b , is included in a 2-plan of equations $x_0 = \frac{\sigma^2}{2\sqrt{2}}$ and $a_i x + b_i y + c_i z = \frac{x_0}{\sigma^2}$.

Proof: \mathcal{F} is the geodesic convex hull in \mathcal{S}^3 of its 20 vertices, so we begin to search the coordinates of the vertices. As the shortest translation distance of the elements of \mathcal{I}^* is $\frac{\pi}{5}$, the shortest translation distance in PDS is $\frac{\pi}{5}$. Two opposite faces must be the image from each other by a Clifford translation with χ equal to $\frac{\pi}{5}$. \mathcal{I}^* has 12 such elements denoted by g_i in the following parts:

$$\frac{1}{2}(\sigma \mathbf{1} + 0 \mathbf{i} \pm \frac{1}{\sigma} \mathbf{j} \pm \mathbf{k}) \text{ (with even permutations of the tree last coordinates).}$$

So the isometries of $SO(3)$ denoted by p_{g_i} leave invariant $p(\mathcal{F}) := \mathcal{F}_v$. Furthermore $(0, 0, 0)$ belongs to \mathcal{F}_v because $(1, 0, 0, 0)$ belongs to \mathcal{F} . So $OB_i := \frac{1}{\sqrt{3-\sigma}}(0, \pm \frac{1}{\sigma}, \pm 1)$, with even permutations, are the orthogonal axes to each pair of opposite faces of \mathcal{F}_v . B_i are the vertices of an icosahedron that is the dual of a regular dodecahedron whose vertices are the barycenters of three equidistant vertices of the icosahedron. We get a pentagonal face having OB_i as symmetry axis by finding the five vertices that are at the same minimal distance from B_i . Among these five points, two vertices are adjacent if they are at a distance inferior or equal from the other vertices of this face. We deduce that, in \mathbb{R}^4 , the last three coordinates of the vertices of \mathcal{F} could be:

$$(\pm \frac{1}{6}\sigma, \pm \frac{1}{6}\sigma, \pm \frac{1}{6}\sigma), \quad \text{or} \quad (0, \pm \frac{1}{6}\sigma^2, \pm \frac{1}{6}) \text{ (with even permutations).}$$

So the coordinates of the 20 vertices C_i belonging to \mathcal{S}^3 and being the vertices of a regular dodecahedron that has the same symmetry axes are of the form:

$$\begin{aligned} & \sqrt{1 - 3(\lambda \frac{\sigma}{6})^2} \mathbf{1} + \lambda(\pm \frac{1}{6}\sigma \mathbf{i} \pm \frac{1}{6}\sigma \mathbf{j} \pm \frac{1}{6}\sigma \mathbf{k}), \\ \text{or} \quad & \sqrt{1 - \lambda^2 \frac{\sigma^2}{12}} \mathbf{1} + \lambda(0 \mathbf{i} \pm \frac{1}{6}\sigma^2 \mathbf{j} \pm \frac{1}{6}\mathbf{k}) \text{ (with even permutations),} \end{aligned}$$

with $\lambda \in \mathbb{R}$ such that two opposite faces can be the image from each other by a Clifford translation with χ equal to $\frac{\pi}{5}$. Consider a face F of \mathcal{F} such that $\frac{1}{2}(-\frac{1}{\sigma}\mathbf{i} - \mathbf{j})$ is a symmetry axis of \mathcal{F}_v orthogonal to the induced face of \mathcal{F}_v . Its adjacent vertices satisfy:

$$\begin{aligned} C_1 &= \sqrt{1 - 3(\lambda \frac{\sigma}{6})^2} \mathbf{1} + \lambda(\frac{1}{6}(-\sigma \mathbf{i} - \sigma \mathbf{j} + \sigma \mathbf{k})), & C_2 &= \sqrt{1 - 3(\lambda \frac{\sigma}{6})^2} \mathbf{1} + \lambda(\frac{1}{6}(-\sigma^2 \mathbf{i} - \mathbf{j})), \\ C_3 &= \sqrt{1 - 3(\lambda \frac{\sigma}{6})^2} \mathbf{1} + \lambda(\frac{1}{6}(-\sigma \mathbf{i} - \sigma \mathbf{j} - \sigma \mathbf{k})), & C_4 &= \sqrt{1 - 3(\lambda \frac{\sigma}{6})^2} \mathbf{1} + \lambda(\frac{1}{6}(-\sigma^2 \mathbf{j} - \mathbf{k})), \\ C_5 &= \sqrt{1 - 3(\lambda \frac{\sigma}{6})^2} \mathbf{1} + \lambda(\frac{1}{6}(-\sigma^2 \mathbf{j} + \mathbf{k})). \end{aligned}$$

And the opposite face having the same symmetry axis has the following adjacent vertices:

$$\begin{aligned} C_6 &= \sqrt{1 - 3(\lambda \frac{\sigma}{6})^2} \mathbf{1} + \lambda(\frac{1}{6}(\sigma \mathbf{i} + \sigma \mathbf{j} - \sigma \mathbf{k})), & C_7 &= \sqrt{1 - 3(\lambda \frac{\sigma}{6})^2} \mathbf{1} + \lambda(\frac{1}{6}(\sigma^2 \mathbf{i} + \mathbf{j})), \\ C_8 &= \sqrt{1 - 3(\lambda \frac{\sigma}{6})^2} \mathbf{1} + \lambda(\frac{1}{6}(\sigma \mathbf{i} + \sigma \mathbf{j} + \sigma \mathbf{k})), & C_9 &= \sqrt{1 - 3(\lambda \frac{\sigma}{6})^2} \mathbf{1} + \lambda(\frac{1}{6}(\sigma^2 \mathbf{j} + \mathbf{k})), \\ C_{10} &= \sqrt{1 - 3(\lambda \frac{\sigma}{6})^2} \mathbf{1} + \lambda(\frac{1}{6}(\sigma^2 \mathbf{j} - \mathbf{k})). \end{aligned}$$

We are searching λ such that C_1 has C_8 as image by the Clifford translation $\frac{1}{2}(\sigma \mathbf{1} + \frac{1}{\sigma} \mathbf{i} + \mathbf{j})$. So the spherical distance between C_1 and C_8 is equal to $\frac{\pi}{5}$. We get $\lambda^2 = \frac{9}{2}(5 - 3\sigma) = \frac{9}{2} \frac{1}{\sigma^4}$. Due to the symmetry of \mathcal{F}_v , the sign of λ is indifferent. So we have found only one $\lambda > 0$ which is suitable for this face. Next we verify that it is also suitable for the others faces. We can then deduce the 20 vertices of \mathcal{F} .

Now we construct the faces of \mathcal{F} . Each of them has five edges which are the shortest geodesic \mathcal{G} joining two adjacent vertices S_i and S_j . The geodesics can be described as follows [16]. A path l on \mathcal{S}^3 is a geodesic if and only if there is a 2-dimensional plane Π in \mathbb{R}^4 passing through the origin such that $l \subset \Pi \cap \mathcal{S}^3$. All the geodesics are circles.

$$\begin{aligned} \text{(III.1)} \quad q \in \mathcal{G} & \iff \exists \alpha \geq 0, \exists \beta \geq 0 \quad q = \alpha OS_i + \beta OS_j \quad \text{and} \quad \|q\| = 1 \\ & \iff \exists \alpha \geq 0, \exists \beta \geq 0 \quad q = \alpha OS_i + \beta OS_j \quad \text{and} \quad 1 = \alpha^2 + \beta^2 + \sigma \alpha \beta. \end{aligned}$$

Then a face is the set of shortest geodesics joining two points of the edges. One may also say that a face is the set of the projection on \mathcal{S}^3 of all barycenters of its five vertices in \mathbb{R}^4 . We note F_i^b the set of all barycenters in \mathbb{R}^4 of the vertices of F_i . It is included in a 2-plan of equations

$x'_0 = \frac{\sigma^2}{2\sqrt{2}}$ and $ax' + by' + cz' = \frac{x'_0}{\sigma^2}$ with even permutations of $(a, b, c) = (\pm\frac{1}{\sigma}, \pm 1, 0)$. As $F_i = \left\{ \frac{1}{\sqrt{x'_0{}^2 + x'^2 + y'^2 + z'^2}}(x'_0, x', y', z'), (x'_0, x', y', z') \in F_i^b \right\}$ we deduce:

$$\forall (x_0, x, y, z) \in F_i, \quad ax + by + cz = \frac{x_0}{\sigma^2}.$$

(See Appendix A for a detailed description of the faces). The proof is complete.

Proposition III.2. *The set of $t(S_i)$ for all t in \mathcal{I}^* , and all S_i of \mathcal{F} has 600 vertices given by:*

- (1) *a set of 24 vertices given by $\frac{1}{2\sqrt{2}}(\pm 2, \pm 2, 0, 0)$ and all its permutations,*
- (2) *a set of 64 vertices given by $\frac{1}{2\sqrt{2}}(\pm\sqrt{5}, \pm 1, \pm 1, \pm 1)$ and all its permutations,*
- (3) *a set of 64 vertices given by $\frac{1}{2\sqrt{2}}(\pm\sigma, \pm\sigma, \pm\sigma, \pm\frac{1}{\sigma^2})$ and all its permutations,*
- (4) *a set of 64 vertices given by $\frac{1}{2\sqrt{2}}(\pm\sigma^2, \pm\frac{1}{\sigma}, \pm\frac{1}{\sigma}, \pm\frac{1}{\sigma})$ and all its permutations,*
- (5) *a set of 96 vertices given by $\frac{1}{2\sqrt{2}}(\sigma^2, \pm\frac{1}{\sigma^2}, 0, \pm 1)$ and all its even permutations,*
- (6) *a set of 96 vertices given by $\frac{1}{2\sqrt{2}}(\pm\sqrt{5}, \pm\frac{1}{\sigma}, 0, \pm\sigma)$ and all its even permutations,*
- (7) *a set of 192 vertices given by $\frac{1}{2\sqrt{2}}(\pm 2, \pm 1, \pm\frac{1}{\sigma}, \pm\sigma)$ and all its even permutations.*

They are the vertices of 120 regular dodecahedra which tessellate \mathcal{S}^3 .

This result is obtained by an explicit calculus of $t(S_i)$ for all t in \mathcal{I}^* and all vertices S_i of \mathcal{F} . Anyone of these regular dodecahedra is a fundamental domain. Following figure 1 shows the three last coordinates of these 600 vertices, viewed from a face of the centered dodecahedron. Straight lines between two vertices symbolize edges of pentagonal faces. We note that these coordinates

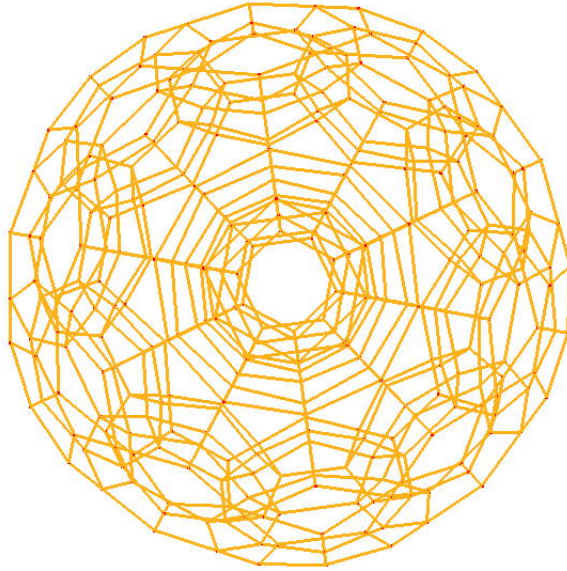


FIGURE 1. 120 Cell

look like those of Coxeter [6], up to an odd permutation of the three last coordinates. They are adapted to \mathcal{I}^* , unlike those of [6]. From proposition III.1 we deduce the following:

Proposition III.3. $p(\mathcal{F})$, denoted \mathcal{F}_v , is a centered regular dodecahedron in \mathbb{R}^3 such that

$$(x, y, z) \in \mathcal{F}_v \iff (+\sqrt{1 - x^2 - y^2 - z^2}, x, y, z) \in \mathcal{F}.$$

It is included in the first ball of the visualization of \mathcal{S}^3 . Its 20 vertices are $\frac{1}{2\sqrt{2}}(\pm\frac{1}{\sigma^2}, 0, \pm 1)$, $\frac{1}{2\sqrt{2}}(0, \pm 1, \pm\frac{1}{\sigma^2})$, $\frac{1}{2\sqrt{2}}(\pm\frac{1}{\sigma}, \pm\frac{1}{\sigma}, \pm\frac{1}{\sigma})$ and $\frac{1}{2\sqrt{2}}(\pm 1, \pm\frac{1}{\sigma^2}, 0)$.

Each face $F_{i,v}$ of \mathcal{F}_v is a regular pentagon included in an ellipsoid

$$F_{i,v} \subset \{(x, y, z) \in \mathbb{R}^3, \sigma^4(ax + by + cz)^2 = 1 - x^2 - y^2 - z^2\}.$$

with (a_i, b_i, c_i) equal to $(\pm\frac{1}{\sigma}, \pm 1, 0)$, up to an even permutation.

The set of all barycenters in \mathbb{R}^3 of the vertices of $F_{i,v}$, denoted by $F_{i,v}^b$, is included in a 2-plan of equation $a_ix + b_iy + c_iz = \frac{1}{2\sqrt{2}}$.

See Appendix A for a detailed description of \mathcal{F}_v . The following figure is a diagramm, and not a visualization, of \mathcal{F} (or \mathcal{F}_v) because their faces are not in a plan of \mathbb{R}^4 (or \mathbb{R}^3).

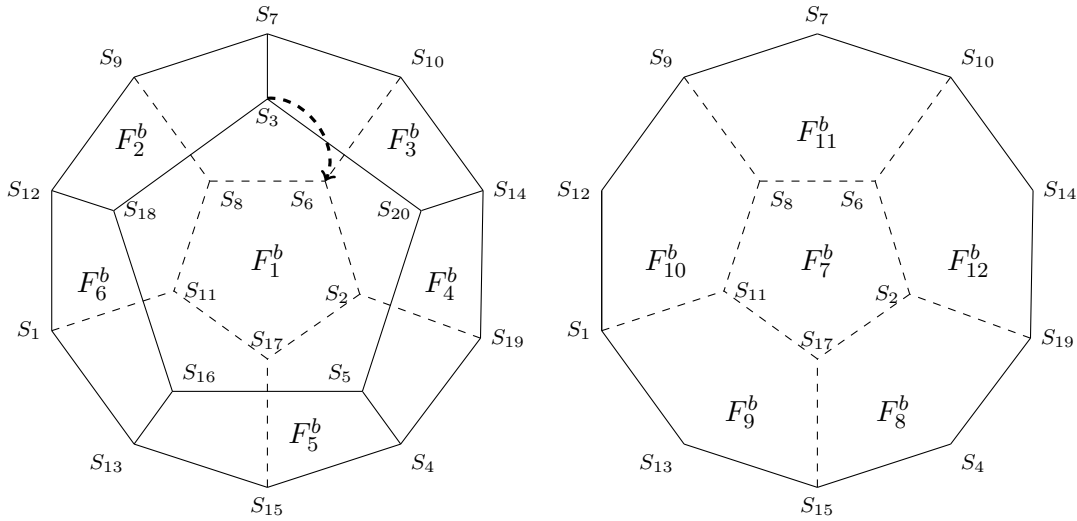


FIGURE 2. Faces $F_{i,b}$ viewed from $F_{1,b}$. The dashed lines are hidden.

IV. EQUIVALENCE RELATIONS ON \mathcal{F} AND \mathcal{F}_v

In order to have relation II.1, the equivalence relation must identify any pentagonal face of \mathcal{F} with its opposite face, after rotating by $\frac{\pi}{5}$ in the clockwise direction around the outgoing axis orthogonal to this last face. First specify our notations. We consider the Clifford translations g_i that have been used for the construction of \mathcal{F} , with:

$$\begin{aligned} g_1 &:= \frac{1}{2}\sigma\mathbf{1} + \frac{1}{2}\frac{1}{\sigma}\mathbf{i} + \frac{1}{2}\mathbf{j}, & g_2 &:= \frac{1}{2}\sigma\mathbf{1} + \frac{1}{2}\mathbf{i} - \frac{1}{2}\frac{1}{\sigma}\mathbf{k}, & g_3 &:= \frac{1}{2}\sigma\mathbf{1} + \frac{1}{2}\frac{1}{\sigma}\mathbf{j} - \frac{1}{2}\mathbf{k}, \\ g_4 &:= \frac{1}{2}\sigma\mathbf{1} - \frac{1}{2}\frac{1}{\sigma}\mathbf{i} + \frac{1}{2}\mathbf{j}, & g_5 &:= \frac{1}{2}\sigma\mathbf{1} + \frac{1}{2}\frac{1}{\sigma}\mathbf{j} + \frac{1}{2}\mathbf{k}, & g_6 &:= \frac{1}{2}\sigma\mathbf{1} + \frac{1}{2}\mathbf{i} + \frac{1}{2}\frac{1}{\sigma}\mathbf{k}. \end{aligned}$$

They are such that: $\forall i \in \{1, \dots, 6\}$, $g_i(F_i) = F_{i+1}$. The inverses of these six first translations are the six other translations:

$$\begin{aligned} g_7 &:= (g_1)^{-1} = \frac{1}{2}\sigma\mathbf{1} - \frac{1}{2}\frac{1}{\sigma}\mathbf{i} - \frac{1}{2}\mathbf{j}, & g_8 &:= (g_2)^{-1} = \frac{1}{2}\sigma\mathbf{1} - \frac{1}{2}\mathbf{i} + \frac{1}{2}\frac{1}{\sigma}\mathbf{k}, & g_9 &:= (g_3)^{-1} = \frac{1}{2}\sigma\mathbf{1} - \frac{1}{2}\frac{1}{\sigma}\mathbf{j} + \frac{1}{2}\mathbf{k}, \\ g_{10} &:= (g_4)^{-1} = \frac{1}{2}\sigma\mathbf{1} + \frac{1}{2}\frac{1}{\sigma}\mathbf{i} - \frac{1}{2}\mathbf{j}, & g_{11} &:= (g_5)^{-1} = \frac{1}{2}\sigma\mathbf{1} - \frac{1}{2}\frac{1}{\sigma}\mathbf{j} - \frac{1}{2}\mathbf{k}, & g_{12} &:= (g_6)^{-1} = \frac{1}{2}\sigma\mathbf{1} - \frac{1}{2}\mathbf{i} - \frac{1}{2}\frac{1}{\sigma}\mathbf{k}. \end{aligned}$$

They all have a translation distance χ equal to $\frac{\pi}{5}$. We have for the vertices (see figure 2 for notations):

$$\begin{aligned} g_1(S_3) &= S_6, & g_1(S_{18}) &= S_8, & g_1(S_{16}) &= S_{11}, & g_1(S_5) &= S_{17}, & g_1(S_{20}) &= S_2, \\ g_2(S_{18}) &= S_{15}, & g_2(S_{12}) &= S_{17}, & g_2(S_9) &= S_2, & g_2(S_7) &= S_{19}, & g_2(S_3) &= S_4, \end{aligned}$$

$$\begin{aligned}
g_3(S_3) &= S_1, & g_3(S_7) &= S_{11}, & g_3(S_{10}) &= S_{17}, & g_3(S_{14}) &= S_{15}, & g_3(S_{20}) &= S_{13}, \\
g_4(S_{20}) &= S_9, & g_4(S_{14}) &= S_8, & g_4(S_{19}) &= S_{11}, & g_4(S_4) &= S_1, & g_4(S_5) &= S_{12}, \\
g_5(S_5) &= S_{10}, & g_5(S_4) &= S_6, & g_5(S_{15}) &= S_8, & g_5(S_{13}) &= S_9, & g_5(S_{16}) &= S_7, \\
g_6(S_{16}) &= S_{19}, & g_6(S_{13}) &= S_2, & g_6(S_1) &= S_6, & g_6(S_{12}) &= S_{10}, & g_6(S_{18}) &= S_{14}.
\end{aligned}$$

We define the relation \sim by specifying the equivalence classes \dot{q} of any $q \in \mathcal{F}$:

$$\forall q \in \mathcal{F}, \quad \dot{q} := \mathcal{I}^*(\{q\}) \cap \mathcal{F}.$$

\mathcal{F} has been constructed such that $\frac{\pi}{5}$ is the translation distance between two opposite faces. Otherwise $\frac{\pi}{5}$ is the smallest translation distance of the elements of \mathcal{I}^* . So:

$$q \in \mathcal{F} \Rightarrow \dot{q} = \left\{ g_i(q), i \in \{1, \dots, 12\} \right\} \cap \mathcal{F}.$$

It follows that:

- If q belongs to $\overset{\circ}{\mathcal{F}}$, then \dot{q} has only one element,
- If q is a vertex of \mathcal{F} , then \dot{q} has four elements,
- If q belongs to an edge of a face, without being a vertex, then \dot{q} has three elements,
- If q belongs to a face and does not belong to an edge, then \dot{q} has two elements.

So we have:

Proposition IV.1. *We define the equivalence classes on \mathcal{F} by:*

$$\begin{aligned}
q \in \overset{\circ}{\mathcal{F}} &\Rightarrow \dot{q} = \{q\}, \\
\exists(i, j, k), q \in F_i \cap F_j \cap F_k &\Rightarrow \dot{q} = \{q, g_i(q), g_j(q), g_k(q)\}, \\
(\exists(i, j), q \in F_i \cap F_j) \text{ and } (\forall k \neq i, j, q \notin F_k) &\Rightarrow \dot{q} = \{q, g_i(q), g_j(q)\}, \\
(\exists i, q \in F_i) \text{ and } (\forall j \neq i, q \notin F_j) &\Rightarrow \dot{q} = \{q, g_i(q)\}.
\end{aligned}$$

Here the integers i, j, k belong to $\{1, \dots, 12\}$.

The equivalence relation \sim on \mathcal{F}_v is easily deduced from this one on \mathcal{F} . Let us denote $g_{i,v}$ the application $\mathbb{R}^3 \rightarrow \mathbb{R}^3$ induced by g_i on \mathcal{F}_v . Hence for all i in $\{1, \dots, 6\}$, $g_{i,v}(F_{i,v}) = F_{i+1,v}$ and $g_{i,v}^{-1} = g_{i+6,v}$. We have:

Proposition IV.2. *We define the equivalence classes on \mathcal{F}_v by:*

$$\begin{aligned}
X \in \overset{\circ}{\mathcal{F}_v} &\Rightarrow \dot{X} = \{X\}, \\
\exists(i, j, k) X \in F_{i,v} \cap F_{j,v} \cap F_{k,v} &\Rightarrow \dot{X} = \{X, g_{i,v}(X), g_{j,v}(X), g_{k,v}(X)\}, \\
(\exists(i, j), X \in F_{i,v} \cap F_{j,v}) \text{ and } (\forall k \neq i, j, X \notin F_{k,v}) &\Rightarrow \dot{X} = \{X, g_{i,v}(X), g_{j,v}(X)\}, \\
(\exists i, X \in F_{i,v}) \text{ and } (\forall j \neq i, X \notin F_{j,v}) &\Rightarrow \dot{X} = \{X, g_{i,v}(X)\}.
\end{aligned}$$

Here the integers i, j, k belong to $\{1, \dots, 12\}$.

The geometrical meaning of this equivalence relation is clear : we identify any pentagonal face of \mathcal{F}_v with its opposite face, after rotating by $\frac{\pi}{5}$ in the clockwise direction around the outgoing axis orthogonal to this last face (see Figure 2).

V. THE WAVE PROPAGATION ON THE DODECAHEDRAL SPACE.

We consider the lorentzian manifold $\mathbb{R}_t \times \mathcal{S}^3/\mathcal{I}^*$ endowed with the metric

$$g_{\mu\nu} dx^\mu dx^\nu = dt^2 - ds_{\mathbf{K}}^2,$$

and we study the scalar covariant wave equation associated to this metric :

$$(V.1) \quad \partial_t^2 \Psi - \Delta_{\mathbf{K}} \Psi = 0.$$

Here $\Delta_{\mathbf{K}}$ is the Laplace Beltrami operator on \mathbf{K} , that is defined by

$$\Delta_{\mathbf{K}} := \frac{1}{\sqrt{|g|}} \partial_{\mu} g^{\mu\nu} \sqrt{|g|} \partial_{\nu}, \quad g^{-1} = (g^{\mu\nu}), \quad |g| = |\det g_{\mu\nu}|.$$

Since \mathbf{K} is a smooth compact manifold without boundary, $-\Delta_{\mathbf{K}}$ endowed with its natural domain $\{u \in L^2(\mathbf{K}); \Delta_{\mathbf{K}} u \in L^2(\mathbf{K})\}$ is a densely defined, positive, self-adjoint operator on $L^2(\mathbf{K})$ and the global Cauchy problem is well posed by the spectral functional calculus :

$$\Psi(t) = \cos(t\sqrt{-\Delta_{\mathbf{K}}}) \Psi(0) + \frac{\sin(t\sqrt{-\Delta_{\mathbf{K}}})}{\sqrt{-\Delta_{\mathbf{K}}}} \partial_t \Psi(0).$$

We shall use the functional framework of the finite energy spaces. Given $m \in \mathbb{N}$, we introduce the Sobolev space

$$H^m(\mathbf{K}) := \{u \in L^2(\mathbf{K}), \nabla_{\mathbf{K}}^{\alpha} u \in L^2(\mathbf{K}), |\alpha| \leq m\}.$$

where $\nabla_{\mathbf{K}}$ are the covariant derivatives. We can also interpret this space as the set of the distributions $u \in H^m(\mathcal{S}^3)$ such that $u \circ g = u$ for any $g \in \mathcal{I}^*$. Then the standard spectral theory assures that for all $\Psi_0 \in H^1(\mathbf{K})$, $\Psi_1 \in L^2(\mathbf{K})$, there exists a unique $\Psi \in C^0(\mathbb{R}_t^+; H^1(\mathbf{K})) \cap C^1(\mathbb{R}_t^+; L^2(\mathbf{K}))$ solution of (V.1) satisfying

$$(V.2) \quad \Psi(t=0) = \Psi_0, \quad \partial_t \Psi(t=0) = \Psi_1,$$

and we have

$$\int_{\mathbf{K}} |\partial_t \Psi(t)|^2 + |\nabla_{\mathbf{K}} \Psi(t)|^2 d\mu_K = Cst.$$

Also we have a result of regularity : when $\Psi_0 \in H^2(\mathbf{K})$, $\Psi_1 \in H^1(\mathbf{K})$, then $\Psi \in C^0(\mathbb{R}_t^+; H^2(\mathbf{K})) \cap C^1(\mathbb{R}_t^+; H^1(\mathbf{K})) \cap C^2(\mathbb{R}_t^+; L^2(\mathbf{K}))$.

Obviously Ψ is entirely determined on $\mathbb{R}_t \times \mathbf{K}$ by its restriction to $\mathbb{R}_t \times \mathcal{F}$. To perform the numerical computation of this solution, we take the domain of visualization $\mathcal{F}_v \subset \mathbb{R}^3$ of the fundamental polygon $\mathcal{F} \subset \mathcal{S}^3$ as the domain of calculus. Therefore we introduce the map f that is one-to-one from \mathcal{F}_v onto \mathcal{F} defined by

$$\begin{aligned} f : \quad \mathcal{F}_v \subset \mathbb{R}^3 &\rightarrow \mathcal{F} \subset \mathcal{S}^3 \\ X = (x, y, z) &\mapsto (\sqrt{1-x^2-y^2-z^2}, x, y, z) = (f_1(x, y, z), f_2(x, y, z), f_3(x, y, z), f_4(x, y, z)), \end{aligned}$$

and we put

$$\psi(t, x, y, z) := \Psi(t, f(x, y, z)).$$

We introduce the usual Sobolev space H^m for the euclidean metric of \mathbb{R}^3 :

$$H^m(\mathcal{F}_v) = \{u \in L^2(\mathcal{F}_v), \forall \alpha \in \mathbb{N}^2, |\alpha| \leq m, \partial_{x,y,z}^{\alpha} u \in L^2(\mathcal{F}_v)\}.$$

Proposition V.1. $\Psi \in C^0(\mathbb{R}_t^+; H^1(\mathbf{K})) \cap C^1(\mathbb{R}_t^+; L^2(\mathbf{K}))$ is solution of (V.1) iff ψ belongs to $C^0(\mathbb{R}_t^+; H^1(\mathcal{F}_v)) \cap C^1(\mathbb{R}_t^+; L^2(\mathcal{F}_v))$ and satisfies the equation

$$(V.3) \quad \partial_{tt} \psi - \Delta_{\mathcal{F}_v} \psi = 0, \quad (t, x, y, z) \in \mathbb{R}^+ \times \mathcal{F}_v,$$

where

$$(V.4) \quad \Delta_{\mathcal{F}_v} = (1-x^2-y^2-z^2) \partial_{11}^2 + (1-y^2) \partial_{22}^2 + (1-z^2) \partial_{33}^2 - 2xy \partial_{12}^2 - 2xz \partial_{13}^2 - 2yz \partial_{23}^2 - 3x \partial_1 - 3y \partial_2 - 3z \partial_3,$$

and the boundary conditions

$$(V.5) \quad \forall (t, X, X') \in \mathbb{R} \times \partial \mathcal{F}_v \times \partial \mathcal{F}_v, \quad X \sim X' \Rightarrow \psi(t, X) = \psi(t, X').$$

Moreover $\Psi \in C^0(\mathbb{R}_t^+; H^2(\mathbf{K})) \cap C^1(\mathbb{R}_t^+; H^1(\mathbf{K})) \cap C^2(\mathbb{R}_t^+; L^2(\mathbf{K}))$ iff $\psi \in C^0(\mathbb{R}_t^+; H^2(\mathcal{F}_v)) \cap C^1(\mathbb{R}_t^+; H^1(\mathcal{F}_v)) \cap C^2(\mathbb{R}_t^+; L^2(\mathcal{F}_v))$.

Proof. We denote g the metric induced on \mathcal{F}_v by the metric of \mathcal{S}^3 and the map f . We get that the coefficients of g_{ij} are:

$$g_{ii} := - \sum_{j=1}^4 f_j(x, y, z) \partial_{ii}^2 f_j(x, y, z),$$

$$g_{ik} := - \sum_{j=1}^4 f_j(x, y, z) \partial_{ik}^2 f_j(x, y, z).$$

So

$$g_{ij} = \begin{pmatrix} \frac{1-y^2-z^2}{1-x^2-y^2-z^2} & \frac{xy}{1-x^2-y^2-z^2} & \frac{xz}{1-x^2-y^2-z^2} \\ \frac{xy}{1-x^2-y^2-z^2} & \frac{1-x^2-z^2}{1-x^2-y^2-z^2} & \frac{yz}{1-x^2-y^2-z^2} \\ \frac{xz}{1-x^2-y^2-z^2} & \frac{yz}{1-x^2-y^2-z^2} & \frac{1-x^2-y^2}{1-x^2-y^2-z^2} \end{pmatrix}, \quad g^{ij} = \begin{pmatrix} 1-x^2 & -xy & -xz \\ -xy & 1-y^2 & -yz \\ -xz & -yz & 1-z^2 \end{pmatrix},$$

and

$$\det g = \frac{1}{1-x^2-y^2-z^2}.$$

As $\Delta_{\mathcal{F}_v} := \frac{1}{\sqrt{|g|}} \partial_\mu g^{\mu\nu} \sqrt{|g|} \partial_\nu$ we obtain the expression of $\Delta_{\mathcal{F}_v}$.

Given $u \in H^1(\mathcal{F}_v)$, the trace of u on \mathcal{F}_v is well defined since the domain \mathcal{F}_v is Lipschitz and C^∞ piecewise. ψ satisfies the boundary conditions (V.5) iff its pull-back Ψ on \mathcal{F} can be extended in a solution defined on the whole Poincaré dodecahedron \mathbf{K} . The extension to the smooth solutions is straightforward. The proof is completed.

To handle the boundary when applying the finite element method, it is very convenient to take into account the boundary condition (V.5) by a suitable choice of the functional space. We introduce the spaces $W^m(\mathcal{F}_v)$ that correspond to the spaces $H^m(\mathbf{K})$:

$$W^0(\mathcal{F}_v) := L^2(\mathcal{F}_v, (1-x^2-y^2-z^2)^{-\frac{1}{2}} dx dy dz),$$

$$1 \leq m, \quad W^m(\mathcal{F}_v) := \left\{ u \in H^m(\mathcal{F}_v), \quad \forall (X, X') \in \partial \mathcal{F}_v^2, \quad X \sim X' \Rightarrow u(X) = u(X') \right\},$$

endowed with the norm

$$\|u\|_{W^m}^2 := \sum_{|\alpha| \leq m} \|\partial^\alpha u\|_{W^0(\mathcal{F}_v)}^2.$$

In particular, we have

$$W^1(\mathcal{F}_v) = \left\{ u \in H^1(\mathcal{F}_v), \quad X \sim X' \Rightarrow u(X) = u(X') \right\},$$

and

$$\psi \in C^k(\mathbb{R}_t, W^m(\mathcal{F}_v)) \iff \Psi \in C^k(\mathbb{R}_t; H^m(\mathbf{K})).$$

The numerical method to solve the Cauchy problem will be based on its variational formulation.

Theorem V.2. *Given $\psi_0 \in W^2(\mathcal{F}_v)$, $\psi_1 \in W^1(\mathcal{F}_v)$, there exists a unique $\psi \in C^0(\mathbb{R}_t^+; W^2(\mathcal{F}_v)) \cap C^1(\mathbb{R}_t^+; W^1(\mathcal{F}_v)) \cap C^2(\mathbb{R}_t^+; W^0(\mathcal{F}_v))$ solution of the equation (V.3), and satisfying*

$$(V.6) \quad \psi(0, \cdot) = \psi_0(\cdot), \quad \partial_t \psi(0, \cdot) = \psi_1(\cdot).$$

ψ is the unique function in $C^0(\mathbb{R}_t^+; W^2(\mathcal{F}_v)) \cap C^1(\mathbb{R}_t^+; W^1(\mathcal{F}_v)) \cap C^2(\mathbb{R}_t^+; W^0(\mathcal{F}_v))$ satisfying (V.6) and such that for any $\phi \in W^1(\mathcal{F}_v)$, we have :

$$(V.7) \quad \begin{aligned} & \frac{d^2}{dt^2} \int_{\mathcal{F}_v} (1 - x^2 - y^2 - z^2)^{-\frac{1}{2}} \psi(t, x, y, z) \phi(x, y, z) dx dy dz \\ & + \int_{\mathcal{F}_v} (1 - x^2 - y^2 - z^2)^{-\frac{1}{2}} \nabla \psi(t, x, y, z) \cdot \nabla \phi(x, y, z) dx dy dz \\ & - \int_{\mathcal{F}_v} (1 - x^2 - y^2 - z^2)^{-\frac{1}{2}} [(x, y, z) \cdot \nabla \psi(t, x, y, z)] [(x, y, z) \cdot \nabla \phi(x, y, z)] dx dy dz = 0. \end{aligned}$$

Proof: The existence and the uniqueness of the solution of the Cauchy problem are given by the previous proposition since the boundary conditions are imposed by our choice of space $W^1(\mathcal{F}_v)$. Now the mixed problem can be expressed as a variational problem. ψ is solution iff for all $\phi \in W^1(\mathcal{F}_v)$, we have :

$$(V.8) \quad \begin{aligned} 0 &= \langle \partial_t^2 \psi - \Delta_{\mathcal{F}_v} \psi; \phi \rangle_{W^0(\mathcal{F}_v)} \\ &= \frac{d^2}{dt^2} \int_{\mathcal{F}_v} \frac{1}{\sqrt{1 - x^2 - y^2 - z^2}} \psi(t, x, y, z) \phi(x, y, z) dx dy dz \\ & \quad - \int_{\mathcal{F}_v} \frac{1}{\sqrt{1 - x^2 - y^2 - z^2}} (\Delta_{\mathcal{F}_v} \psi)(t, x, y, z) \phi(x, y, z) dx dy dz. \end{aligned}$$

To get the formulation (V.7), the key point consists in expressing in a symetric manner the last integral, without using an integral on the boundary. To invoke the Green formula, we denote $\nu(x, y, z)$ the unit outgoing normal at (x, y, z) belonging to face $F_{i,v}$. We know explicit form of $g_{i,v}$, the application $\mathbb{R}^3 \rightarrow \mathbb{R}^3$ induced by g_i on \mathcal{F}_v . Thanks to relations written in Appendix A, we have:

$$\begin{aligned} g_{1,v}(x, y, z) &= \frac{1}{2} \begin{pmatrix} \frac{1}{\sigma} & -\sigma & 1 \\ -\sigma & -1 & -\frac{1}{\sigma} \\ -1 & \frac{1}{\sigma} & \sigma \end{pmatrix} \begin{pmatrix} x \\ y \\ z \end{pmatrix}, & g_{2,v}(x, y, z) &= \frac{1}{2} \begin{pmatrix} -1 & \frac{1}{\sigma} & \sigma \\ -\frac{1}{\sigma} & \sigma & -1 \\ -\sigma & 1 & \frac{1}{\sigma} \end{pmatrix} \begin{pmatrix} x \\ y \\ z \end{pmatrix}, \\ g_{3,v}(x, y, z) &= \frac{1}{2} \begin{pmatrix} \sigma & 1 & \frac{1}{\sigma} \\ -1 & \frac{1}{\sigma} & \sigma \\ -\frac{1}{\sigma} & \sigma & -1 \end{pmatrix} \begin{pmatrix} x \\ y \\ z \end{pmatrix}, & g_{4,v}(x, y, z) &= \frac{1}{2} \begin{pmatrix} \frac{1}{\sigma} & \sigma & 1 \\ \sigma & -1 & \frac{1}{\sigma} \\ -1 & -\frac{1}{\sigma} & \sigma \end{pmatrix} \begin{pmatrix} x \\ y \\ z \end{pmatrix}, \\ g_{5,v}(x, y, z) &= \frac{1}{2} \begin{pmatrix} \sigma & -1 & \frac{1}{\sigma} \\ 1 & \frac{1}{\sigma} & -\sigma \\ -\frac{1}{\sigma} & -\sigma & -1 \end{pmatrix} \begin{pmatrix} x \\ y \\ z \end{pmatrix}, & g_{6,v}(x, y, z) &= \frac{1}{2} \begin{pmatrix} -1 & -\frac{1}{\sigma} & -\sigma \\ \frac{1}{\sigma} & \sigma & -1 \\ -\sigma & 1 & \frac{1}{\sigma} \end{pmatrix} \begin{pmatrix} x \\ y \\ z \end{pmatrix}. \end{aligned}$$

Moreover we know $\nu(x, y, z)$ thanks to the equation of the ellipsoids (Appendix A). We verify that:

$$g_{i,v}(\nu(x, y, z)) = -\nu(g_{i,v}(x, y, z)),$$

Since $(u \circ g_{i,v})|_{F_{i,v}} = u|_{F_{i,v}}$, we have for $u \in W^2(\mathcal{F}_v)$

$$\partial_{\nu(X)} u(x, y, z) = g_{i,v}[\nu(x, y, z)] \cdot \nabla u(g_{i,v}(x, y, z)) = -\partial_{\nu(g_{i,v}(x, y, z))} u(g_{i,v}(x, y, z)).$$

We deduce that for $u \in W^2(\mathcal{F}_v)$, $v \in W^1(\mathcal{F}_v)$, we have

$$\begin{aligned} \int_{F_{i,v}} v(x, y, z) \partial_{\nu(x, y, z)} u d\sigma(x, y, z) &= - \int_{g_{i,v}(F_{i,v})} v(x, y, z) \partial_{\nu(x, y, z)} u d\sigma(x, y, z) \\ &= - \int_{F_{i+6,v}} v(x, y, z) \partial_{\nu(x, y, z)} u d\sigma(x, y, z), \end{aligned}$$

and therefore

$$\int_{\partial \mathcal{F}_v} v(x, y, z) \partial_{\nu(x, y, z)} u d\sigma(x, y, z) = 0,$$

where $d\sigma$ denotes the volume measure on $(\partial\mathcal{F}_v, g)$. We conclude that :

$$\int_{\mathcal{F}_v} (\Delta_{\mathcal{F}_v} \psi)(t, x, y, z) \phi(x, y, z) \sqrt{\det g} \, dx \, dy \, dz = - \int_{\mathcal{F}_v} g(\text{grad } \psi, \text{grad } \phi) \sqrt{\det g} \, dx \, dy \, dz.$$

To simplify the writing we shall note in the following X instead of (x, y, z) and $|X|^2$ instead of $x^2 + y^2 + z^2$ for $(x, y, z) \in \mathcal{F}_v$; and dX will designate $dx \, dy \, dz$. Therefore we compute :

$$\begin{aligned} & \int_{\mathcal{F}_v} (1 - |X|^2)^{-\frac{1}{2}} \Delta_{\mathcal{F}_v} \psi(t, X) \phi(X) \, dX = \\ & - \int_{\mathcal{F}_v} (1 - |X|^2)^{-\frac{1}{2}} \left[(1 - x^2) \partial_1 \psi(t, X) \partial_1 \phi(t, X) + (1 - y^2) \partial_2 \psi(t, X) \partial_2 \phi(t, X) + (1 - z^2) \partial_3 \psi(t, X) \partial_3 \phi(t, X) \right] \, dX \\ & + \int_{\mathcal{F}_v} (1 - |X|^2)^{-\frac{1}{2}} \left[xy (\partial_1 \psi(t, X) \partial_2 \phi(t, X) + \partial_2 \psi(t, X) \partial_1 \phi(t, X)) + xz (\partial_1 \psi(t, X) \partial_3 \phi(t, X) + \partial_3 \psi(t, X) \partial_1 \phi(t, X)) \right. \\ & \quad \left. + yz (\partial_2 \psi(t, X) \partial_3 \phi(t, X) + \partial_3 \psi(t, X) \partial_2 \phi(t, X)) \right] \, dX. \end{aligned}$$

And finally we calculate :

$$\begin{aligned} & \int_{\mathcal{F}_v} (1 - |X|^2)^{-\frac{1}{2}} \Delta_{\mathcal{F}_v} \psi(t, X) \phi(X) \, dX = \\ & - \int_{\mathcal{F}_v} (1 - |X|^2)^{-\frac{1}{2}} \nabla \psi(t, X) \cdot \nabla \phi(t, X) \, dX + \int_{\mathcal{F}_v} (1 - |X|^2)^{-\frac{1}{2}} (X \cdot \nabla \psi(t, X)) (X \cdot \nabla \phi(t, X)) \, dX. \end{aligned}$$

The proof of the theorem is complete.

We solve this variational problem by the usual way. We take a family V_h , $0 < h \leq h_0$, of finite dimensional vector subspaces of $W^1(\mathcal{F}_v)$. We assume that

$$\overline{\cup_{0 < h \leq h_0} V_h} = W^1(\mathcal{F}_v).$$

We choose sequences $\psi_{0,h}, \psi_{1,h} \in V_h$ such that

$$\psi_{0,h} \rightarrow \psi_0 \text{ in } W^1(\mathcal{F}_v), \quad \psi_{1,h} \rightarrow \psi_1 \text{ in } L^2(\mathcal{F}_v).$$

We consider the solution $\psi_h \in C^\infty(\mathbb{R}_t; V_h)$ of

$$\begin{aligned} \forall \phi_h \in V_h, \quad & \frac{d^2}{dt^2} \int_{\mathcal{F}_v} (1 - |X|^2)^{-\frac{1}{2}} \psi_h(t, X) \phi_h(X) \, dX + \int_{\mathcal{F}_v} (1 - |X|^2)^{-\frac{1}{2}} \nabla \psi_h(t, X) \cdot \nabla \phi_h(t, X) \, dX \\ & - \int_{\mathcal{F}_v} (1 - |X|^2)^{-\frac{1}{2}} (X \cdot \nabla \psi_h(t, X)) (X \cdot \nabla \phi_h(t, X)) \, dX = 0, \end{aligned}$$

satisfying $\psi_h(0, \cdot) = \psi_{0,h}(\cdot)$, $\partial_t \psi_h(0, \cdot) = \psi_{1,h}(\cdot)$. Thanks to the conservation of the energy,

$$\int_{\mathcal{F}_v} (|\partial_t \psi(t, x, y, z)|^2 + |\nabla_{\mathcal{F}_v} \psi(t, x, y, z)|^2) \sqrt{\det g} \, dx \, dy \, dz = Cst,$$

this scheme is stable :

$$\forall T > 0, \quad \sup_{0 < h \leq h_0} \sup_{0 \leq t \leq T} \|\psi_h(t)\|_{W^1} + \left\| \frac{d}{dt} \psi_h(t) \right\|_{L^2} < \infty.$$

Moreover, when $\psi \in C^2(\mathbb{R}_t^+; W^1(\mathcal{F}_v))$, it is also converging :

$$\forall T > 0, \quad \sup_{0 \leq t \leq T} \|\psi_h(t) - \psi(t)\|_{W^1} + \left\| \frac{d}{dt} \psi_h(t) - \frac{d}{dt} \psi(t) \right\|_{L^2} \rightarrow 0, \quad h \rightarrow 0.$$

If we take a basis $(e_j^h)_{1 \leq j \leq N_h}$ of V_h , we expand ψ_h on this basis :

$$\psi_h(t) = \sum_{j=1}^{N_h} \psi_j^h(t) e_j^h,$$

and we introduce

$$U(t) := {}^t(\psi_1^h, \psi_2^h, \dots, \psi_{N_h}^h)$$

$$\mathbb{M} = (M_{ij})_{1 \leq i, j \leq N_h}, \quad \mathbb{D} = (D_{ij})_{1 \leq i, j \leq N_h}, \quad \mathbb{K} = (K_{ij})_{1 \leq i, j \leq N_h}$$

$$M_{ij} := \int_{\mathcal{F}_v} \frac{1}{\sqrt{1 - |X|^2}} e_i^h(X) e_j^h(X) dX,$$

$$K_{ij} := \int_{\mathcal{F}_v} \frac{1}{\sqrt{1 - |X|^2}} (\partial_x e_i^h(X) \partial_x e_j^h(X) + \partial_y e_i^h(X) \partial_y e_j^h(X) + \partial_z e_i^h(X) \partial_z e_j^h(X)) dX.$$

$$D_{ij} := - \int_{\mathcal{F}_v} \frac{1}{\sqrt{1 - |X|^2}} (x \partial_x e_i^h(X) + y \partial_y e_i^h(X) + z \partial_z e_i^h(X)) (x \partial_x e_j^h(X) + y \partial_y e_j^h(X) + z \partial_z e_j^h(X)) dX.$$

Then the variational formulation is equivalent to

$$\mathbb{M}X'' + (\mathbb{K} + \mathbb{D})X = 0.$$

This differential system is solved very simply by iteration by solving

$$\mathbb{M}(U^{n+1} - 2U^n + U^{n-1}) + (\Delta T)^2 (\mathbb{K} + \mathbb{D})U^n = 0.$$

We know that this scheme is stable, and so convergent by the Lax theorem, when

$$\sup_{U \neq 0} \frac{\langle (\mathbb{K} + \mathbb{D})U, U \rangle}{\langle \mathbb{M}U, U \rangle} < \frac{4}{\Delta T^2}.$$

Therefore if there exists $K > 0$ such that

$$\forall h \in]0, h_0], \quad \forall \phi_h \in V_h, \quad \left\| \frac{\nabla_{x,y,z} \phi_h}{(1 - |X|^2)^{\frac{1}{4}}} \right\|_{L^2(\mathcal{F}_v)} \leq \frac{K}{h} \left\| \frac{\phi_h}{(1 - |X|^2)^{\frac{1}{4}}} \right\|_{L^2(\mathcal{F}_v)},$$

the CFL condition

$$K \Delta T < \sqrt{2}h,$$

is sufficient to assure the stability and the convergence of our scheme.

VI. NUMERICAL RESOLUTION

VI.1. Mesh. Our goal is to build a mesh of $\partial\mathcal{F}$ such that it has a fixed size in advance, all the edges are splitting in the same way, and the meshes of two opposite faces are the image from each other by the Clifford translation g_i fitting for \sim . Of course we also want that all points of the mesh of $F_{i,v} \subset \partial\mathcal{F}$ are on the suitable ellipsoid, and that all points of the edges of $F_{i,v}$ are on the right geodesic.

First of all we construct the boundary $\partial\mathcal{F}_v$. Each F_i^b is included in a 2-plan of \mathbb{R}^4 and can be easily meshed with a convenient metric. We choose to build a mesh of F_1^b , with $F_1 := (S_3, S_{18}, S_{16}, S_5, S_{20})$. We denote $F_{1,v}^b := p(F_1^b)$ the visualization of F_1^b . As we want the vertices on each edge of F_1 are equidistant, we choose *a priori* the desired spherical distance between two consecutive vertices. This determines the number of vertices on an edge. Then, by a suitable application, we map F_1^b in the 2-plan $z = 0$ of \mathbb{R}^3 , which allows us to use a 2-D mesh generator able to respect a given metric matrix M . Let us recall the inclusions

$$F_1^b \subset \left\{ (x_0, x, y, z) \in \mathbb{R}^4, \quad x_0 = \frac{\sigma^2}{2\sqrt{2}}, \quad -\frac{1}{\sigma}x - y = \frac{x_0}{\sigma^2} \right\},$$

$$F_{1,v}^b \subset \left\{ (x, y, z) \in \mathbb{R}^3, \quad -\frac{1}{\sigma}x - y = \frac{1}{2\sqrt{2}} \right\}.$$

We do a translation t of $F_{1,v}^b$ by the vector $\overrightarrow{OM_{5,20}} = (0, -\frac{1}{\sqrt{2}}, 0)$ where $M_{5,20}$ denotes the middle of $S_5 S_{20}$, followed by a rotation r in \mathbb{R}^3 , with an angle $-\frac{\pi}{2}$ and axis $\vec{u} = \overrightarrow{S_{18}M_{5,20}} = (\frac{1}{\sqrt{3-\sigma}}, -\frac{1}{\sigma\sqrt{3-\sigma}}, 0)$. So, thanks to the quaternionic calculus:

$$r(x\mathbf{i} + y\mathbf{j} + z\mathbf{k}) = \left[\frac{1}{\sqrt{2}}\mathbf{1} - \frac{1}{\sqrt{2}} \left(\frac{1}{\sqrt{3-\sigma}}\mathbf{i} - \frac{\sqrt{2}}{2} \frac{1}{\sigma\sqrt{3-\sigma}}\mathbf{j} \right) \right] [x\mathbf{i} + y\mathbf{j} + z\mathbf{k}] \left[\frac{1}{\sqrt{2}}\mathbf{1} + \frac{1}{\sqrt{2}} \left(\frac{1}{\sqrt{3-\sigma}}\mathbf{i} - \frac{\sqrt{2}}{2} \frac{1}{\sigma\sqrt{3-\sigma}}\mathbf{j} \right) \right],$$

and,

$$r(x, y, z) = \begin{pmatrix} \frac{1}{3-\sigma}x - \frac{1}{\sigma(3-\sigma)}y + \frac{1}{\sigma\sqrt{3-\sigma}}z \\ -\frac{1}{\sigma(3-\sigma)}x + \frac{1}{\sigma^2(3-\sigma)}y + \frac{1}{\sqrt{3-\sigma}}z \\ -\frac{1}{\sigma\sqrt{3-\sigma}}x - \frac{1}{\sqrt{3-\sigma}}y \end{pmatrix}.$$

If (x, y, z) belongs to $F_{1,v}^b$ we get

$$(r \circ t)(x, y, z) = \left(x', y', -\frac{1}{\sigma\sqrt{3-\sigma}}x - \frac{1}{\sqrt{3-\sigma}} \left(y + \frac{1}{2\sqrt{2}} \right) \right) = (x', y', 0).$$

Therefore $r \circ t(F_{1,v}^b)$ is in the 2-plan $z = 0$ of \mathbb{R}^3 . Of course we want a metric on \mathbb{R}^2 endowed by the metric of \mathcal{S}^3 . We denote by f the application that maps $r \circ t(F_{1,v}^b)$ to F_1 , that is f :

$$\begin{array}{ccccc} r \circ t(F_{1,v}^b) & \rightarrow & \mathbb{R}^3 & \rightarrow & F_{1,v}^b & \rightarrow & F_1^b \subset \mathbb{R}^4 \\ (x, y) & \mapsto & (x, y, 0) & \mapsto & (x', y', z') := (r \circ t)^{-1}(x, y, 0) & \mapsto & \left(\frac{\sigma^2}{2\sqrt{2}}, x', y', z' \right) \end{array}$$

followed by:

$$\begin{array}{ccc} F_1^b \subset \mathbb{R}^4 & \rightarrow & F_1 \subset \mathcal{S}^3 \\ \left(\frac{\sigma^2}{2\sqrt{2}}, x', y', z' \right) & \mapsto & \frac{1}{\left\| \left(\frac{\sigma^2}{2\sqrt{2}}, x', y', z' \right) \right\|} \left(\frac{\sigma^2}{2\sqrt{2}}, x', y', z' \right). \end{array}$$

We deduce that the coefficients of M are given by:

$$(VI.1) \quad m_{ii} := - \sum_{j=1,4} f_j(x, y) \partial_{ii}^2 f_j(x, y), \quad m_{ik} := - \sum_{j=1,4} f_j(x, y) \partial_{ik}^2 f_j(x, y).$$

See Appendix B for the values m_{ij} .

We used the software FreeFem++ ([8]) for the generation of the 2-D mesh of $r \circ t(F_{1,v}^b)$. Then, applying f , we get a mesh of F_1 with the wanted size. Moreover, as we know the equation of the 2-plan containing $F_{1,v}^b$, we are able to control and to correct the coordinates of the vertices of the mesh of $F_{1,v}^b$ with a great precision. We can also control and correct that the vertices on the edges of F_1 are on the convenient geodesic (III.1), distant from each other with the wanted distance.

Then, by the use of rotations in \mathbb{R}^3 we get a mesh of the five adjacent faces $F_{2,v}^b, \dots, F_{6,v}^b$ (see Appendix C). After normalizing we have got a mesh of F_1, \dots, F_6 . At last, by the use of g_1, \dots, g_6 we deduce a mesh of F_7, \dots, F_{12} . Once more we control and correct the vertices on edges. As we also know the equation of the ellipsoid that contains each face, we also control all the vertices. Meshes of each $F_{i,v}$ are obtained from those of F_i by discarding the first coordinate of the vertices.

To get the mesh of \mathcal{F} we used the software Tetgen ([18]) in several ways. We have created a mesh with an inner sphere or an inner dodecahedron, in order to impose two different average sizes of tetrahedra depending on the location. We also used Tetgen with a *.mtr* file that gives us the wanted size near each point. In all cases we employed an option so that there is no point introduced into $\partial\mathcal{F}_v$.

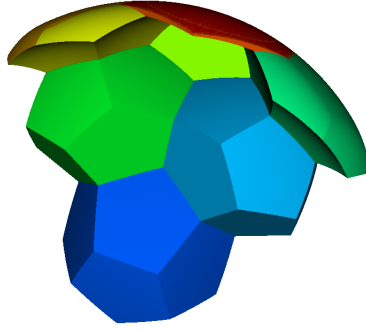
We can see the accuracy of our mesh by calculating the sum of the volume of tetrahedra which compose \mathcal{F}_v . This sum must be closed to $\frac{2\pi^2}{120}$ that is $\simeq 0.1644934066$.

Mesh	number of vertices	number of nodes	number of tetrahedra	sum	relative error
$F089$	182162	730309	4642744	0.1644927119	$4,22E-006$
$F101$	233858	1600118	10198710	0.1644928648	$3,29E-006$

The minimal and maximal distances between two vertices of the bounder of these meshes are:

Mesh	minimal	maximal
$F089$	$2.06E-003$	$6.11E-003$
$F101$	$1.82E-003$	$4.90E-003$

We can also look at the tilling of \mathcal{S}^3 . In figure 3 we display six images of \mathcal{F}_v , as well as \mathcal{F} in the first ball of visualization of \mathcal{S}^3 . All points of theses images have a positive first coordinate in \mathbb{R}^4 , except those of $g_2 g_1 g_1(\mathcal{F})$. To fully represent this last set, we should also draw the second ball of visualization of \mathcal{S}^3 , in which its representation is the same as in the first ball.



■ \mathcal{F}_v , ■ $g_1(\mathcal{F}_v)$, ■ $g_1 g_1(\mathcal{F}_v)$, ■ $g_6(\mathcal{F}_v)$, ■ $g_6 g_6(\mathcal{F}_v)$, ■ $g_5 g_6(\mathcal{F}_v)$, ■ $g_2 g_1 g_1(\mathcal{F}_v)$

FIGURE 3. The Fundamental Domain (dark blue) and six images of it.

VI.2. V_h space. We construct the finite element spaces V_h of \mathbb{P}_1 type. We take into account the boundary condition (V.5) in the definition of the finite elements, so that $V_h \subset W^1(\mathcal{F}_v)$. We note \mathcal{T}_h all tetrahedra of a mesh, and $\mathcal{F}_{v,h} = \cup_{K \in \mathcal{T}_h} K$. Then we introduce :

$$V_h := \left\{ v : \mathcal{F}_{v,h} \rightarrow \mathbb{R}, v \in \mathcal{C}^0(\mathcal{F}_{v,h}), \forall K \in \mathcal{T}_h, v|_K \in \mathbb{P}_1(K), M \sim M' \Rightarrow v(M) = v(M') \right\}.$$

The equivalent points on $\partial\mathcal{F}_v$ are known thanks our construction of meshes. The number of nodes N_h is the sum of $\frac{30}{3} \times nbve + \frac{12}{2} \times nbvf + nbvi + \frac{20}{4}$, with $nbve$ the number of vertices on an edge of a face that are not a vertex of \mathcal{F}_v , $nbvf$ the number of vertices on a face that are not on an edge, $nbvi$ the number of vertices in $\mathring{\mathcal{F}}_v$.

If j is the number of a node and if M_i denotes a vertex of the mesh, we construct a basis $(e_j^h)_{1 \leq j \leq N_h}$ of V_h by:

- (1) If j is associated to a node that does not belong to $\partial\mathcal{F}_v$: $e_j^h(M_i) = \delta_{ij}$.
There are $nbvi$ functions of this kind.

- (2) If j is associated to a node that is a vertex of \mathcal{F}_v :

$$e_j^h(M_i) = \begin{cases} 1 & \text{if } M_i \sim M_j, \\ 0 & \text{otherwise.} \end{cases}$$

There are five functions of this kind.

- (3) If j is associated to a node that belongs to a face of $\partial\mathcal{F}_v$ and not to an edge:

$$e_j^h(M_i) = \begin{cases} 1 & \text{if } M_i = P_i, \\ 0 & \text{otherwise.} \end{cases}$$

There are $6 \times nbvf$ functions of this kind.

- (4) If j is associated to a node that belongs to an edge of a face of $\partial\mathcal{F}_v$ and is not a vertex of

$$\mathcal{F}_v: e_j^h(M_i) = \begin{cases} 1 & \text{if } M_i = P_i, \\ 0 & \text{otherwise.} \end{cases}$$

There are $10 \times nbve$ functions of this last kind.

VI.3. Matrix form of the problem. $\mathbb{K}(i, j)$, $\mathbb{D}(i, j)$ and $\mathbb{M}(i, j)$ are found with a numerical integration using CUBPACK ([4]). These matrices are sparse and symetric. So we choose a Morse storage of their lower part, and all of the calculations will be performed with this storage. To solve the linear problem we use a preconditioned conjugate gradient method. The preconditioner is an incomplete Choleski factorisation, and the starting point is the solution obtained with a diagonal preconditioner.

VI.4. Initial data. We choose different initial data. Some of them have a more or less small support near given points, others are chosen randomly. For the wave depicted in figure 4, we have taken

$$\psi_0(X) = 100e^{\frac{d(X, X_0)}{d(X, X_0) - r_0}}, \text{ for } d(X, X_0) \leq r_0, \text{ and } \psi_0(X) = 0, \text{ for } d(X, X_0) \geq r_0.$$

with $X_0 = (0, 0, 0)$ and $r_0 = 0.3$. In the following we refer to as the name $Init_c$. And for the one depicted in figure 6, we have taken a similar function with a smaller support, and especially a support not centered at the origin. In the following we refer to as the name $Init_{exc}$.

VI.5. Time resolution. In order to see the stability of our method, we compute $E_d(t)$, the discretized energy at the time t :

$$E(n\Delta t) = \left\langle \mathbb{M} \frac{X^n - X^{n-1}}{\Delta t}, \frac{X^n - X^{n-1}}{\Delta t} \right\rangle + \left\langle (\mathbb{K} + \mathbb{D}) X^{n-1}, X^n \right\rangle.$$

It is well known that our scheme is conservative, hence E_d must be invariant all along the resolution: this is the case. For example, with the previous initial data and the use of the mesh $F089$, we obtain:

Initial data	$E_d(0)$	$E_d(80)$
$Init_c$	9328.34990491949	9328.34990491958
$Init_{exc}$	6248.87928527422	6248.87928527418

Here are some characteristic pictures for a centered initial data. At each time there are a view of the solution on $\partial\mathcal{F}_v$, and on a cutting plane ($z = 0$).

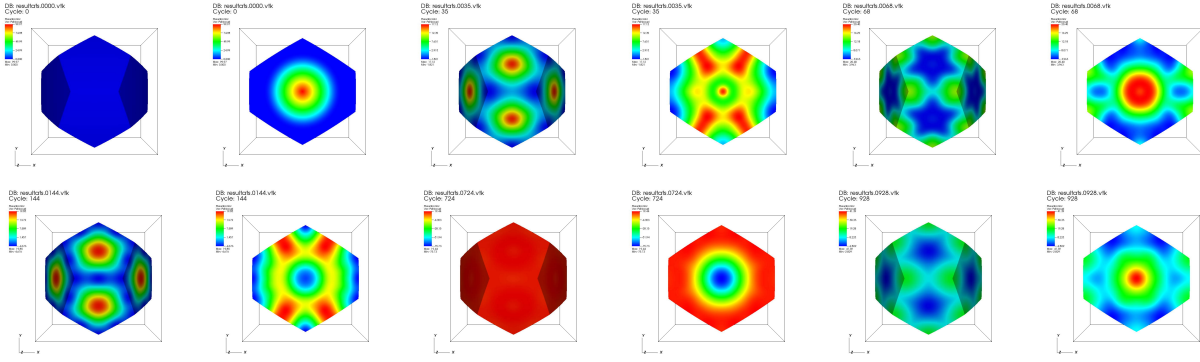


FIGURE 4. A transient wave at $t = 0, t = 2.8, t = 5.44, t = 11.52, t = 57.92, t = 74.24$.

The solution varies extremely fast as you can see on the next picture. This was expected since eigenvalues are large.

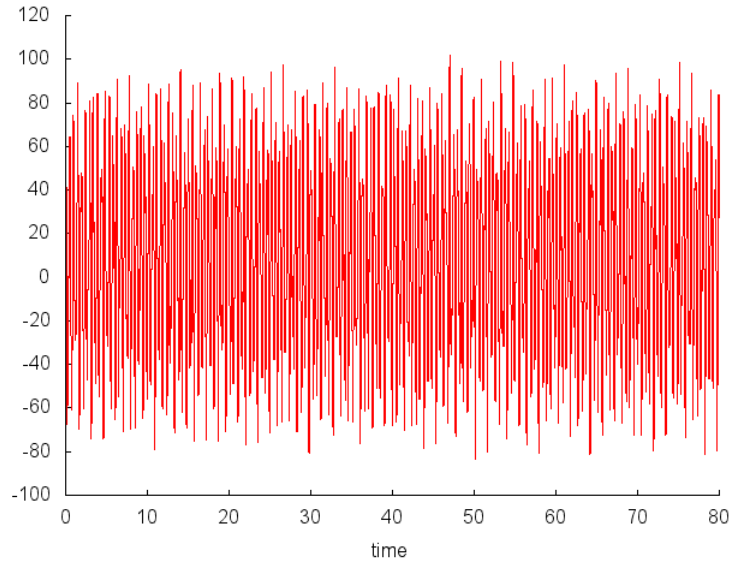


FIGURE 5. The solution $\psi(t, X_0)$ from $t = 0$ to $t = 80$.

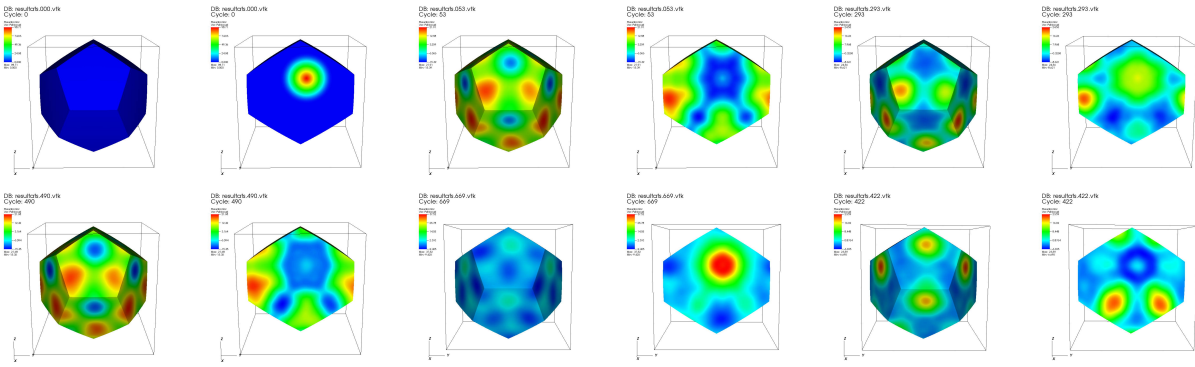


FIGURE 6. Another transient wave at $t = 0, t = 2.65, t = 14.65, t = 24.5, t = 33.45, t = 71.10$.

Some movies are available on this personal home-page ².

VI.6. Eigenvalues. We test our scheme in the time domain, by looking for the eigenvalues that are explicitly known (see [1], [9], [10], [11]). Since the Laplace-Beltrami operator $\Delta_{\mathbf{K}}$ on PDS is a non positive, self-adjoint elliptic operator on a compact manifold, its spectrum is a discrete set of eigenvalues $-q^2 \leq 0$, and by the Hilbert-Schmidt theorem, there exists an orthonormal basis in $L^2(\mathbf{K})$, formed of eigenfunctions $(\psi_q)_q \subset H^\infty(\mathbf{K})$ associated to q^2 , i.e.

$$-\Delta_{\mathcal{F}_v} \psi_q = q^2 \psi_q, \quad \psi_q \in W^\infty(\mathcal{F}_v).$$

One has:

$$q^2 = \beta^2 - 1,$$

with $\beta \in \{1, 13, 21, 25, 31, 33, 37, 41, 43, 45, 49, 51, 53, 55, 57\} \cup \{2n+1, n \geq 30\}$, and we take $\psi_0 = \frac{1}{2\sqrt{\pi}}$. Therefore any finite energy solution $\psi(t, X)$ of $\partial_t^2 \psi - \Delta_{\mathbf{K}} \psi = 0$ has an expansion of the form $\sum_q e^{iqt} \psi_q(X)$. More precisely, if we denote \langle, \rangle the scalar product in $L^2(\mathbf{K})$, we write

$$\begin{aligned} \psi(t, X) = & \frac{1}{4\pi} (\langle \partial_t \psi(0, \cdot), 1 \rangle t + \langle \psi(0, \cdot), 1 \rangle) \\ & + \sum_{q \neq 0} \langle \partial_t \psi(0, \cdot), \psi_q \rangle \frac{\sin qt}{q} \psi_q(x, y) + \langle \psi(0, \cdot), \psi_q \rangle \cos qt \psi_q(X). \end{aligned}$$

To compute the eigenvalues q^2 we investigate the Fourier transform in time of the signal $\psi(t, X_0)$ in the case where $\partial_t \psi(0, X) = 0$, for different X_0 . Practically, during the time resolution of the equation, we store the values of the solution at some vertices $M(X)$ for the discrete time $k\Delta t$, $N_i \leq k \leq N_f$. We choose the initial step N_i in order to the transient wave is stabilized, that to say $N_i \Delta t$ is at least greater than the diameter of \mathcal{F}_v , i.e. $N_i \Delta t \geq 2 * d(0, S_1) = d(S_1, S_{14}) = \arccos\left(\frac{3\sigma-2}{8}\right) \simeq 0.776279$. Then we compute a DFT of $(\psi_h(k\Delta t, X))_{N_i \leq k \leq N_f}$ with the free FFT library `fftw3`. After we search the values $jmax_1, jmax_2, \dots$ for which the previous result $(\Psi_j(X))_{0, N_f - N_i + 1}$ has a maximum. The eigenvalues found by the algorithm are expressed as:

$$q = \frac{2\pi}{(N_f - N_i + 1)\Delta t} jmax.$$

We have made tests by varying parameters such as: N_i , mesh, initial data. In almost all cases we have obtained the 36 first consecutive eigenvalues with an relative error of about 10^{-2} . For example here are non zero values found with the mesh F089, $Init_{exc}$ as initial data, and $\Delta t = 0.0005$. FFT is performed from $N_i = 1800$ to $N_f = 106770$.

²<http://www.math.u-bordeaux1.fr/~mbachelo/PDS.html>

β	exact q^2	numerical result	relative error	β	exact q^2	numerical result	relative error
13	168	167.6126	$2.3060753E-03$	69	4760	4871.141	$2.3348872E-02$
21	440	438.8956	$2.5100708E-03$	71	5040	5171.347	$2.6060946E-02$
25	624	628.4641	$7.1539269E-03$	73	5328	5463.117	$2.5359832E-02$
31	960	965.4485	$5.6755068E-03$	75	5624	5762.894	$2.4696665E-02$
33	1088	1093.790	$5.3216149E-03$	77	5928	6089.032	$2.7164599E-02$
37	1368	1374.492	$4.7458406E-03$	79	6240	6424.146	$2.9510655E-02$
41	1680	1696.904	$1.0062009E-02$	81	6560	6787.617	$3.4697667E-02$
43	1848	1865.750	$9.6047800E-03$	83	6888	7121.304	$3.3871040E-02$
45	2024	2042.602	$9.1906162E-03$	85	7224	7462.999	$3.3083960E-02$
49	2400	2431.920	$1.3299967E-02$	87	7568	7833.520	$3.5084505E-02$
51	2600	2633.263	$1.2793344E-02$	89	7920	8213.017	$3.6997046E-02$
53	2808	2842.612	$1.2326320E-02$	91	8280	8536.121	$3.0932499E-02$
55	3024	3059.969	$1.1894347E-02$	93	8648	8601.490	$5.3780950E-03$
57	3248	3298.837	$1.5651835E-02$	95	9024	8645.207	$4.1976172E-02$
61	3720	3789.000	$1.8548321E-02$	97	9408	8954.335	$4.8221201E-02$
63	3968	4039.324	$1.7974915E-02$	99	9800	9021.282	$7.9461001E-02$
65	4224	4297.656	$1.7437559E-02$	101	10200	9405.365	$7.7905372E-02$
67	4488	4579.910	$2.0479091E-02$	103	10608	9797.453	$7.6409020E-02$

VI.7. Conclusion. We note a good agreement of the eigenvalues obtained by the spectral analysis of the transient waves that we have computed. We emphasize that this result is a strong evidence of the accuracy of our numerical approximation since the waves are rapidly oscillating due to the large value of the eigenvalues. Therefore we conclude that we have validated this computational method of the waves on the Poincaré dodecahedral space, and we plan to extend it, in the future, to the case of the non-linear waves on this manifold.

VII. APPENDICES

VII.1. **Appendix A.** Description of \mathcal{F} and \mathcal{F}_v .

(1) Coordinates of the vertices S_i of \mathcal{F} :

$$\begin{aligned} S_1 &= \frac{1}{2\sqrt{2}} \left(\sigma^2, -\frac{1}{\sigma}, \frac{1}{\sigma}, -\frac{1}{\sigma} \right), & S_2 &= \frac{1}{2\sqrt{2}} \left(\sigma^2, 1, \frac{1}{\sigma^2}, 0 \right), & S_3 &= \frac{1}{2\sqrt{2}} \left(\sigma^2, -\frac{1}{\sigma}, -\frac{1}{\sigma}, \frac{1}{\sigma} \right), & S_4 &= \frac{1}{2\sqrt{2}} \left(\sigma^2, \frac{1}{\sigma}, -\frac{1}{\sigma}, -\frac{1}{\sigma} \right), \\ S_5 &= \frac{1}{2\sqrt{2}} \left(\sigma^2, 0, -1, -\frac{1}{\sigma^2} \right), & S_6 &= \frac{1}{2\sqrt{2}} \left(\sigma^2, \frac{1}{\sigma}, \frac{1}{\sigma}, \frac{1}{\sigma} \right), & S_7 &= \frac{1}{2\sqrt{2}} \left(\sigma^2, -\frac{1}{\sigma^2}, 0, 1 \right), & S_8 &= \frac{1}{2\sqrt{2}} \left(\sigma^2, 0, 1, \frac{1}{\sigma^2} \right), \\ S_9 &= \frac{1}{2\sqrt{2}} \left(\sigma^2, -\frac{1}{\sigma}, \frac{1}{\sigma}, \frac{1}{\sigma} \right), & S_{10} &= \frac{1}{2\sqrt{2}} \left(\sigma^2, \frac{1}{\sigma^2}, 0, 1 \right), & S_{11} &= \frac{1}{2\sqrt{2}} \left(\sigma^2, 0, 1, -\frac{1}{\sigma^2} \right), & S_{12} &= \frac{1}{2\sqrt{2}} \left(\sigma^2, -1, \frac{1}{\sigma^2}, 0 \right), \\ S_{13} &= \frac{1}{2\sqrt{2}} \left(\sigma^2, -\frac{1}{\sigma^2}, 0, -1 \right), & S_{14} &= \frac{1}{2\sqrt{2}} \left(\sigma^2, \frac{1}{\sigma}, -\frac{1}{\sigma}, \frac{1}{\sigma} \right), & S_{15} &= \frac{1}{2\sqrt{2}} \left(\sigma^2, \frac{1}{\sigma^2}, 0, -1 \right), & S_{16} &= \frac{1}{2\sqrt{2}} \left(\sigma^2, -\frac{1}{\sigma}, -\frac{1}{\sigma}, -\frac{1}{\sigma} \right), \\ S_{17} &= \frac{1}{2\sqrt{2}} \left(\sigma^2, \frac{1}{\sigma}, \frac{1}{\sigma}, -\frac{1}{\sigma} \right), & S_{18} &= \frac{1}{2\sqrt{2}} \left(\sigma^2, -1, -\frac{1}{\sigma^2}, 0 \right), & S_{19} &= \frac{1}{2\sqrt{2}} \left(\sigma^2, 1, -\frac{1}{\sigma^2}, 0 \right), & S_{20} &= \frac{1}{2\sqrt{2}} \left(\sigma^2, 0, -1, \frac{1}{\sigma^2} \right). \end{aligned}$$

(2) Images by the Clifford translation g_i of the face F_i of \mathcal{F} and of its edges.

g_1 maps F_1 to F_7 , and we have for the vertices and the edges:

$$\begin{aligned} g_1(S_3) &= S_6, \quad g_1(S_{18}) = S_8, \quad g_1(S_{16}) = S_{11}, \quad g_1(S_5) = S_{17}, \quad g_1(S_{20}) = S_2, \\ g_1(\widehat{S_3 S_{18}}) &= \widehat{S_6 S_8}, \quad g_1(\widehat{S_{18} S_{16}}) = \widehat{S_8 S_{11}}, \quad g_1(\widehat{S_{16} S_5}) = \widehat{S_{11} S_{17}}, \quad g_1(\widehat{S_5 S_{20}}) = \widehat{S_{17} S_2}, \\ g_1(\widehat{S_{20} S_3}) &= \widehat{S_2 S_6}. \end{aligned}$$

g_2 maps F_2 to F_8 , and we have for the vertices and the edges:

$$\begin{aligned} g_2(S_{18}) &= S_{15}, \quad g_2(S_{12}) = S_{17}, \quad g_2(S_9) = S_2, \quad g_2(S_7) = S_{19}, \quad g_2(S_3) = S_4, \\ g_2(\widehat{S_{18} S_{12}}) &= \widehat{S_{15} S_{17}}, \quad g_2(\widehat{S_{17} S_2}) = \widehat{S_8 S_{11}}, \quad g_2(\widehat{S_9 S_7}) = \widehat{S_2 S_{19}}, \quad g_2(\widehat{S_7 S_3}) = \widehat{S_{19} S_4}, \\ g_2(\widehat{S_3 S_{18}}) &= \widehat{S_4 S_{15}}. \end{aligned}$$

g_3 maps F_3 to F_9 , and we have for the vertices and the edges:

$$\begin{aligned} g_3(S_3) &= S_1, \quad g_3(S_7) = S_{11}, \quad g_3(S_{10}) = S_{17}, \quad g_3(S_{14}) = S_{15}, \quad g_3(S_{20}) = S_{13}, \\ g_3(\widehat{S_3 S_7}) &= \widehat{S_1 S_{11}}, \quad g_3(\widehat{S_7 S_{10}}) = \widehat{S_{11} S_{17}}, \quad g_3(\widehat{S_{10} S_{14}}) = \widehat{S_{17} S_{15}}, \quad g_3(\widehat{S_{14} S_{20}}) = \widehat{S_{15} S_{13}}, \\ g_3(\widehat{S_{20} S_3}) &= \widehat{S_{13} S_1}. \end{aligned}$$

g_4 maps F_4 to F_{10} , and we have for the vertices and the edges:

$$\begin{aligned} g_4(S_{20}) &= S_9, \quad g_4(S_{14}) = S_8, \quad g_4(S_{19}) = S_{11}, \quad g_4(S_4) = S_1, \quad g_4(S_5) = S_{12}, \\ g_4(\widehat{S_{20} S_{14}}) &= \widehat{S_9 S_8}, \quad g_4(\widehat{S_{14} S_{19}}) = \widehat{S_8 S_{11}}, \quad g_4(\widehat{S_{19} S_4}) = \widehat{S_{11} S_1}, \quad g_4(\widehat{S_4 S_5}) = \widehat{S_1 S_{12}}, \\ g_4(\widehat{S_5 S_{20}}) &= \widehat{S_{12} S_9}. \end{aligned}$$

g_5 maps F_5 to F_{11} , and we have for the vertices and the edges:

$$\begin{aligned} g_5(S_5) &= S_{10}, \quad g_5(S_4) = S_6, \quad g_5(S_{15}) = S_8, \quad g_5(S_{13}) = S_9, \quad g_5(S_{16}) = S_7, \\ g_5(\widehat{S_5 S_4}) &= \widehat{S_{10} S_6}, \quad g_5(\widehat{S_4 S_{15}}) = \widehat{S_6 S_8}, \quad g_5(\widehat{S_{15} S_{13}}) = \widehat{S_8 S_9}, \quad g_5(\widehat{S_{13} S_{16}}) = \widehat{S_9 S_7}, \\ g_5(\widehat{S_{16} S_5}) &= \widehat{S_7 S_{10}} \end{aligned}$$

g_6 maps F_6 to F_{12} , and we have for the vertices and the edges:

$$\begin{aligned} g_6(S_{16}) &= S_{19}, \quad g_6(S_{13}) = S_2, \quad g_6(S_1) = S_6, \quad g_6(S_{12}) = S_{10}, \quad g_6(S_{18}) = S_{14}, \\ g_6(\widehat{S_{16} S_{13}}) &= \widehat{S_{19} S_2}, \quad g_6(\widehat{S_{13} S_1}) = \widehat{S_2 S_6}, \quad g_6(\widehat{S_1 S_{12}}) = \widehat{S_6 S_{10}}, \quad g_6(\widehat{S_{12} S_{18}}) = \widehat{S_{10} S_{14}}, \\ g_6(\widehat{S_{18} S_{16}}) &= \widehat{S_{14} S_{19}}. \end{aligned}$$

- (3) F_i^b , the set of all barycenters in \mathbb{R}^4 of the vertices of F_i , is included in a 2-plan of \mathbb{R}^4 . There are the equations of these 2-plans.

$$\begin{aligned} F_1^b &\subset \left\{ (x_0, x, y, z) \in \mathbb{R}^4, x_0 = \frac{\sigma^2}{2\sqrt{2}}, -\frac{1}{\sigma}x - y = \frac{x_0}{\sigma^2} \right\}, & F_7^b &\subset \left\{ (x_0, x, y, z) \in \mathbb{R}^4, x_0 = \frac{\sigma^2}{2\sqrt{2}}, +\frac{1}{\sigma}x + y = \frac{x_0}{\sigma^2} \right\}, \\ F_2^b &\subset \left\{ (x_0, x, y, z) \in \mathbb{R}^4, x_0 = \frac{\sigma^2}{2\sqrt{2}}, -x + \frac{1}{\sigma}z = \frac{x_0}{\sigma^2} \right\}, & F_8^b &\subset \left\{ (x_0, x, y, z) \in \mathbb{R}^4, x_0 = \frac{\sigma^2}{2\sqrt{2}}, +x - \frac{1}{\sigma}z = \frac{x_0}{\sigma^2} \right\}, \\ F_3^b &\subset \left\{ (x_0, x, y, z) \in \mathbb{R}^4, x_0 = \frac{\sigma^2}{2\sqrt{2}}, -\frac{1}{\sigma}y + z = \frac{x_0}{\sigma^2} \right\}, & F_9^b &\subset \left\{ (x_0, x, y, z) \in \mathbb{R}^4, x_0 = \frac{\sigma^2}{2\sqrt{2}}, +\frac{1}{\sigma}y - z = \frac{x_0}{\sigma^2} \right\}, \\ F_4^b &\subset \left\{ (x_0, x, y, z) \in \mathbb{R}^4, x_0 = \frac{\sigma^2}{2\sqrt{2}}, +\frac{1}{\sigma}x - y = \frac{x_0}{\sigma^2} \right\}, & F_{10}^b &\subset \left\{ (x_0, x, y, z) \in \mathbb{R}^4, x_0 = \frac{\sigma^2}{2\sqrt{2}}, -\frac{1}{\sigma}x + y = \frac{x_0}{\sigma^2} \right\}, \\ F_5^b &\subset \left\{ (x_0, x, y, z) \in \mathbb{R}^4, x_0 = \frac{\sigma^2}{2\sqrt{2}}, -\frac{1}{\sigma}y - z = \frac{x_0}{\sigma^2} \right\}, & F_{11}^b &\subset \left\{ (x_0, x, y, z) \in \mathbb{R}^4, x_0 = \frac{\sigma^2}{2\sqrt{2}}, +\frac{1}{\sigma}y + z = \frac{x_0}{\sigma^2} \right\}, \\ F_6^b &\subset \left\{ (x_0, x, y, z) \in \mathbb{R}^4, x_0 = \frac{\sigma^2}{2\sqrt{2}}, -x - \frac{1}{\sigma}z = \frac{x_0}{\sigma^2} \right\}, & F_{12}^b &\subset \left\{ (x_0, x, y, z) \in \mathbb{R}^4, x_0 = \frac{\sigma^2}{2\sqrt{2}}, +x + \frac{1}{\sigma}z = \frac{x_0}{\sigma^2} \right\}. \end{aligned}$$

- (4) So, after having normalized the points of F_i^b , we get that F_i is included in an hyperplan of \mathbb{R}^4 . There are the equations of these 3-plans.

$$\begin{aligned} F_1 &\subset \left\{ (x_0, x, y, z) \in \mathcal{S}^3, -\frac{1}{\sigma}x - y = \frac{x_0}{\sigma^2} \right\}, & F_7 &\subset \left\{ (x_0, x, y, z) \in \mathcal{S}^3, +\frac{1}{\sigma}x + y = \frac{x_0}{\sigma^2} \right\}, \\ F_2 &\subset \left\{ (x_0, x, y, z) \in \mathcal{S}^3, -x + \frac{1}{\sigma}z = \frac{x_0}{\sigma^2} \right\}, & F_8 &\subset \left\{ (x_0, x, y, z) \in \mathcal{S}^3, +x - \frac{1}{\sigma}z = \frac{x_0}{\sigma^2} \right\}, \\ F_3 &\subset \left\{ (x_0, x, y, z) \in \mathcal{S}^3, -\frac{1}{\sigma}y + z = \frac{x_0}{\sigma^2} \right\}, & F_9 &\subset \left\{ (x_0, x, y, z) \in \mathcal{S}^3, +\frac{1}{\sigma}y - z = \frac{x_0}{\sigma^2} \right\}, \\ F_4 &\subset \left\{ (x_0, x, y, z) \in \mathcal{S}^3, +\frac{1}{\sigma}x - y = \frac{x_0}{\sigma^2} \right\}, & F_{10} &\subset \left\{ (x_0, x, y, z) \in \mathcal{S}^3, -\frac{1}{\sigma}x + y = \frac{x_0}{\sigma^2} \right\}, \\ F_5 &\subset \left\{ (x_0, x, y, z) \in \mathcal{S}^3, -\frac{1}{\sigma}y - z = \frac{x_0}{\sigma^2} \right\}, & F_{11} &\subset \left\{ (x_0, x, y, z) \in \mathcal{S}^3, +\frac{1}{\sigma}y + z = \frac{x_0}{\sigma^2} \right\}, \\ F_6 &\subset \left\{ (x_0, x, y, z) \in \mathcal{S}^3, -x - \frac{1}{\sigma}z = \frac{x_0}{\sigma^2} \right\}, & F_{12} &\subset \left\{ (x_0, x, y, z) \in \mathcal{S}^3, +x + \frac{1}{\sigma}z = \frac{x_0}{\sigma^2} \right\}. \end{aligned}$$

- (5) We deduce from the previous items that $F_{i,v}^b$, the set of all barycenters in \mathbb{R}^3 of the vertices of $F_{i,v}$, is included in a plan of \mathbb{R}^3 . There are the equations of these plans.

$$\begin{aligned} F_{1,v}^b &\subset \left\{ (x, y, z) \in \mathbb{R}^3, -\frac{1}{\sigma}x - y = \frac{1}{2\sqrt{2}} \right\}, & F_{7,v}^b &\subset \left\{ (x, y, z) \in \mathbb{R}^3, +\frac{1}{\sigma}x + y = \frac{1}{2\sqrt{2}} \right\}, \\ F_{2,v}^b &\subset \left\{ (x, y, z) \in \mathbb{R}^3, -x + \frac{1}{\sigma}z = \frac{1}{2\sqrt{2}} \right\}, & F_{8,v}^b &\subset \left\{ (x, y, z) \in \mathbb{R}^3, +x - \frac{1}{\sigma}z = \frac{1}{2\sqrt{2}} \right\}, \\ F_{3,v}^b &\subset \left\{ (x, y, z) \in \mathbb{R}^3, -\frac{1}{\sigma}y + z = \frac{1}{2\sqrt{2}} \right\}, & F_{9,v}^b &\subset \left\{ (x, y, z) \in \mathbb{R}^3, +\frac{1}{\sigma}y - z = \frac{1}{2\sqrt{2}} \right\}, \\ F_{4,v}^b &\subset \left\{ (x, y, z) \in \mathbb{R}^3, +\frac{1}{\sigma}x - y = \frac{1}{2\sqrt{2}} \right\}, & F_{10,v}^b &\subset \left\{ (x, y, z) \in \mathbb{R}^3, -\frac{1}{\sigma}x + y = \frac{1}{2\sqrt{2}} \right\}, \\ F_{5,v}^b &\subset \left\{ (x, y, z) \in \mathbb{R}^3, -\frac{1}{\sigma}y - z = \frac{1}{2\sqrt{2}} \right\}, & F_{11,v}^b &\subset \left\{ (x, y, z) \in \mathbb{R}^3, +\frac{1}{\sigma}y + z = \frac{1}{2\sqrt{2}} \right\}, \\ F_{6,v}^b &\subset \left\{ (x, y, z) \in \mathbb{R}^3, -x - \frac{1}{\sigma}z = \frac{1}{2\sqrt{2}} \right\}, & F_{12,v}^b &\subset \left\{ (x, y, z) \in \mathbb{R}^3, +x + \frac{1}{\sigma}z = \frac{1}{2\sqrt{2}} \right\}. \end{aligned}$$

- (6) As $x_0^2 = 1 - x^2 - y^2 - z^2$, we obtain from item 4 that the faces $F_{i,v}$ of \mathcal{F}_v are included in an ellipsoid.

$$\begin{aligned} F_{1,v} \text{ and } F_{7,v} &\text{ are included in the same ellipsoid } \{(x, y, z) \in \mathbb{R}^3, (\sigma + 2)x^2 + 3\sigma^2y^2 + z^2 + 2\sigma^3xy = 1\}. \\ F_{2,v} \text{ and } F_{8,v} &\text{ are included in the same ellipsoid } \{(x, y, z) \in \mathbb{R}^3, 3\sigma^2x^2 + y^2 + (\sigma + 2)z^2 - 2\sigma^3xz = 1\}. \\ F_{3,v} \text{ and } F_{9,v} &\text{ are included in the same ellipsoid } \{(x, y, z) \in \mathbb{R}^3, x^2 + (\sigma + 2)y^2 + 3\sigma^2z^2 - 2\sigma^3yz = 1\}. \\ F_{4,v} \text{ and } F_{10,v} &\text{ are included in the same ellipsoid } \{(x, y, z) \in \mathbb{R}^3, (\sigma + 2)x^2 + 3\sigma^2y^2 + z^2 - 2\sigma^3xy = 1\}. \\ F_{5,v} \text{ and } F_{11,v} &\text{ are included in the same ellipsoid } \{(x, y, z) \in \mathbb{R}^3, x^2 + (\sigma + 2)y^2 + 3\sigma^2z^2 + 2\sigma^3yz = 1\}. \\ F_{6,v} \text{ and } F_{12,v} &\text{ are included in the same ellipsoid } \{(x, y, z) \in \mathbb{R}^3, 3\sigma^2x^2 + y^2 + (\sigma + 2)z^2 + 2\sigma^3xz = 1\}. \end{aligned}$$

VII.2. Appendix B. We give the expression of the metric matrix on \mathbb{R}^2 endowed by the metric of \mathcal{S}^3 which is written in VI.1. We denote by f the application that transforms the 2-D mesh in a mesh of F_1 , that is f :

$$\begin{aligned} \mathbb{R}^2 &\rightarrow \mathbb{R}^3 &\rightarrow F_{1,v}^b \subset \mathbb{R}^3 &\rightarrow F_1^b \subset \mathbb{R}^4 &\rightarrow F_1 \subset \mathcal{S}^3 \\ (x, y) &\mapsto (x, y, 0) &\mapsto (x', y', z') := (r \circ t)^{-1}(x, y, 0) &\mapsto \left(\frac{\sigma^2}{2\sqrt{2}}, x', y', z' \right) &\mapsto \frac{1}{\left\| \left(\frac{\sigma^2}{2\sqrt{2}}, x', y', z' \right) \right\|} \left(\frac{\sigma^2}{2\sqrt{2}}, x', y', z' \right) \end{aligned}$$

We simplify:

$$\left\| \left(\frac{\sigma^2}{2\sqrt{2}}, x', y', z' \right) \right\|^2 = \frac{5}{20^2} [80x^2 + 80y^2 + 8\sqrt{2}\sqrt{5}x + \sqrt{2}(20 + 4\sqrt{5})y + 45 + 17\sqrt{5}] := \frac{g(x, y)}{20^2}.$$

So:

$$\begin{aligned} f_1 &:= (x, y) \mapsto \frac{5}{2} \frac{\sqrt{2}(3+\sqrt{5})}{\sqrt{g(x, y)}}, \\ f_2 &:= (x, y) \mapsto \frac{(10+2\sqrt{5})x-4\sqrt{5}y-\sqrt{10}}{\sqrt{g(x, y)}}, \\ f_3 &:= (x, y) \mapsto \frac{1}{2} \frac{-8\sqrt{5}x+(20-4\sqrt{5})y-(5+\sqrt{5})\sqrt{2}}{\sqrt{g(x, y)}}, \\ f_4 &:= (x, y) \mapsto \frac{\sqrt{5+\sqrt{5}}((5-\sqrt{5})\sqrt{2}x+2\sqrt{10}y+\sqrt{5})}{\sqrt{g(x, y)}}. \end{aligned}$$

Thanks to Maple we obtain:

$$\begin{aligned} m_{11} &:= 320 [80x^2 + 80y^2 + 8\sqrt{2}\sqrt{5}x + 20\sqrt{2}y + 4\sqrt{2}\sqrt{5}y + 45 + 17\sqrt{5}]^{-3} \\ &\times [1600x^2y^2 + 1600y^4 + 80\sqrt{2}\sqrt{5}x^2y + 400\sqrt{2}x^2y + 160\sqrt{2}\sqrt{5}xy^2 + 800\sqrt{2}y^3 + 160\sqrt{2}\sqrt{5}y^3 \\ &+ 860x^2 + 340\sqrt{5}x^2 + 80xy + 80\sqrt{5}xy + 760\sqrt{5}y^2 + 2000y^2 + 86\sqrt{2}\sqrt{5}x \\ &+ 170\sqrt{2}x + 258\sqrt{2}\sqrt{5}y + 610\sqrt{2}y + 845 + 374\sqrt{5}], \\ m_{22} &:= 160 [80x^2 + 80y^2 + 8\sqrt{2}\sqrt{5}x + 20\sqrt{2}y + 4\sqrt{2}\sqrt{5}y + 45 + 17\sqrt{5}]^{-3} \\ &\times [3200x^4 + 3200x^2y^2 + 640\sqrt{2}\sqrt{5}x^3 + 800\sqrt{2}x^2y + 160\sqrt{2}\sqrt{5}x^2y + 320\sqrt{5}\sqrt{2}xy^2 + 3800x^2 \\ &+ 1320\sqrt{5}x^2 + 160\sqrt{5}xy + 160xy + 1680y^2 + 640\sqrt{5}y^2 + 660\sqrt{2}x + 348\sqrt{2}\sqrt{5}x + 244\sqrt{2}\sqrt{5}y \\ &+ 580\sqrt{2}y + 717\sqrt{5} + 1625], \\ m_{12} &:= 32000 [80x^2 + 80y^2 + 8\sqrt{2}\sqrt{5}x + 20\sqrt{2}y + 4\sqrt{2}\sqrt{5}y + 45 + 17\sqrt{5}]^{-6} \\ &\times [8192000x^9y + 32768000x^7y^3 + 49152000x^5y^5 + 32768000x^3y^7 + 8192000xy^9 + 204800\sqrt{2}\sqrt{5}x^9 \\ &+ 1024000\sqrt{2}x^9 + 3686400\sqrt{2}\sqrt{5}x^8y + 2457600\sqrt{5}\sqrt{2}x^7y^2 + 12288000\sqrt{2}x^7y^2 + 11468800\sqrt{2}\sqrt{5}x^6y^3 \\ &+ 6144000\sqrt{5}\sqrt{2}x^5y^4 + 30720000\sqrt{2}x^5y^4 + 12288000\sqrt{2}\sqrt{5}x^4y^5 + 5734400\sqrt{5}\sqrt{2}x^3y^6 \\ &+ 28672000\sqrt{2}x^3y^6 + 4915200\sqrt{5}\sqrt{2}x^2y^7 + 9216000\sqrt{2}xy^8 + 1843200\sqrt{5}\sqrt{2}xy^8 + 409600\sqrt{5}\sqrt{2}y^9 \\ &+ 921600x^8 + 921600\sqrt{5}x^8 + 7782400\sqrt{5}x^7y + 27443200x^7y + 8601600x^6y^2 + 8601600\sqrt{5}x^6y^2 \\ &+ 84787200x^5y^3 + 25804800\sqrt{5}x^5y^3 + 15360000\sqrt{5}x^4y^4 + 15360000x^4y^4 + 87244800x^3y^5 \\ &+ 28262400\sqrt{5}x^3y^5 + 8601600x^2y^6 + 8601600\sqrt{5}x^2y^6 + 29900800xy^7 + 10240000\sqrt{5}xy^7 + 921600\sqrt{5}y^8 \\ &+ 921600y^8 + 1495040\sqrt{2}\sqrt{5}x^7 + 3993600\sqrt{2}x^7 + 7884800\sqrt{2}\sqrt{5}x^6y + 13619200\sqrt{2}x^6y \\ &+ 13578240\sqrt{2}\sqrt{5}x^5y^2 + 35328000\sqrt{2}x^5y^2 + 18329600\sqrt{2}\sqrt{5}x^4y^3 + 32256000\sqrt{2}x^4y^3 \\ &+ 22835200\sqrt{2}\sqrt{5}x^3y^4 + 57856000\sqrt{2}x^3y^4 + 11857920\sqrt{2}\sqrt{5}x^2y^5 + 21196800\sqrt{2}x^2y^5 + 26521600\sqrt{2}xy^6 \\ &+ 10752000\sqrt{2}\sqrt{5}xy^6 + 1413120\sqrt{5}\sqrt{2}y^7 + 2560000\sqrt{2}y^7 + 4802560x^6 + 2365440\sqrt{5}x^6 + 43054080x^5y \\ &+ 18201600\sqrt{5}x^5y + 31795200x^4y^2 + 15513600\sqrt{5}x^4y^2 + 95078400x^3y^3 + 40704000\sqrt{5}x^3y^3 \\ &+ 15820800\sqrt{5}x^2y^4 + 32716800x^2y^4 + 51655680xy^5 + 22379520\sqrt{5}xy^5 + 5232640y^6 + 2508800\sqrt{5}y^6 \\ &+ 2740224\sqrt{2}\sqrt{5}x^5 + 6259200\sqrt{2}x^5 + 19347200\sqrt{2}x^4y + 8878336\sqrt{2}\sqrt{5}x^4y + 16392192\sqrt{2}\sqrt{5}x^3y^2 \\ &+ 37248000\sqrt{2}x^3y^2 + 27302400\sqrt{2}x^2y^3 + 12486144\sqrt{2}\sqrt{5}x^2y^3 + 13570048\sqrt{2}\sqrt{5}xy^4 + 30681600\sqrt{2}xy^4 \\ &+ 5241600\sqrt{2}y^5 + 2389248\sqrt{2}\sqrt{5}y^5 + 5671424x^4 + 2559744\sqrt{5}x^4 + 32037888x^3y + 14255616\sqrt{5}x^3y \\ &+ 9666048\sqrt{5}x^2y^2 + 21451776x^2y^2 + 36815872xy^3 + 16409088\sqrt{5}xy^3 + 6244864y^4 + 2809600\sqrt{5}y^4 \\ &+ 1914304\sqrt{2}\sqrt{5}x^3 + 4288192\sqrt{2}x^3 + 8825088\sqrt{2}x^2y + 3954816\sqrt{2}\sqrt{5}x^2y + 5696448\sqrt{5}\sqrt{2}xy^2 \\ &+ 12752064\sqrt{2}xy^2 + 3657984\sqrt{2}y^3 + 1638528\sqrt{2}\sqrt{5}y^3 + 2327712x^2 + 1041696\sqrt{5}x^2 + 3759032\sqrt{5}xy \\ &+ 8408152xy + 1119072\sqrt{5}y^2 + 2501088y^2 + 458214\sqrt{2}\sqrt{5}x + 1024706\sqrt{2}x + 357278\sqrt{2}\sqrt{5}y \\ &+ 798798\sqrt{2}y + 192091 + 85909\sqrt{5}]. \end{aligned}$$

VII.3. **Appendix C.** We present the rotations that map $F_{1,v}^b$ to each $F_{i,v}^b$ for i belonging to $\{2, 6\}$. Using them, we can build a mesh of the five adjacent faces $F_{2,v}^b, \dots, F_{6,v}^b$ of $F_{1,v}^b$.

• $F_{1,v}^b$ is sent to $F_{6,v}^b$ and $F_{3,v}^b$ by rotations in \mathbb{R}^3 with an angle $\pm \frac{2\pi}{5}$ and an axis $\vec{u} := \frac{1}{\|\vec{OG}_2\|} \vec{OG}_2$, where G_2 denotes the center of $F_{2,v}^b$. We have: $\vec{u} = \frac{1}{\sqrt{5}\sqrt{2+\sigma}} (-(\sigma+2)\mathbf{i} + \sqrt{5}\mathbf{k})$. It is easier to calculate a rotation with an angle equal to $\frac{4\pi}{5}$ than with an angle equal to $\frac{2\pi}{5}$. Hence we begin to calculate ρ a rotation in \mathbb{R}^3 with an angle $\frac{4\pi}{5}$ and an axis \vec{u} :

$$\begin{aligned} \rho \quad (x\mathbf{i} + y\mathbf{j} + z\mathbf{k}) &= \left[\cos\left(\frac{2\pi}{5}\right) \mathbf{1} + \sin\left(\frac{2\pi}{5}\right) \vec{u} \right] [x\mathbf{i} + y\mathbf{j} + z\mathbf{k}] \left[\cos\left(\frac{2\pi}{5}\right) \mathbf{1} - \sin\left(\frac{2\pi}{5}\right) \vec{u} \right] \\ &= \left[\frac{1}{2\sigma} \mathbf{1} + \frac{\sqrt{2+\sigma}}{2} \frac{1}{\sqrt{5}\sqrt{2+\sigma}} (-(2+\sigma)\mathbf{i} + \sqrt{5}\mathbf{k}) \right] [x\mathbf{i} + y\mathbf{j} + z\mathbf{k}] \left[\frac{1}{2\sigma} \mathbf{1} - \frac{\sqrt{2+\sigma}}{2} \frac{1}{\sqrt{5}\sqrt{2+\sigma}} (-(2+\sigma)\mathbf{i} + \sqrt{5}\mathbf{k}) \right]. \end{aligned}$$

So

$$\rho(x, y, z) = \frac{1}{2} \begin{pmatrix} 1 & -\frac{1}{\sigma} & -\sigma \\ \frac{1}{\sigma} & -\sigma & 1 \\ -\sigma & -1 & -\frac{1}{\sigma} \end{pmatrix} \begin{pmatrix} x \\ y \\ z \end{pmatrix}.$$

Hence $\rho^2 : F_{1,v}^b \rightarrow F_{6,v}^b$, and $\rho^3 : F_{1,v}^b \rightarrow F_{3,v}^b$. We have:

$$\rho^2(x, y, z) = \frac{1}{2} \begin{pmatrix} \sigma & 1 & -\frac{1}{\sigma} \\ -1 & \frac{1}{\sigma} & -\sigma \\ -\frac{1}{\sigma} & \sigma & 1 \end{pmatrix} \begin{pmatrix} x \\ y \\ z \end{pmatrix}, \quad \rho^3(x, y, z) = \frac{1}{2} \begin{pmatrix} \sigma & -1 & -\frac{1}{\sigma} \\ 1 & \frac{1}{\sigma} & \sigma \\ -\frac{1}{\sigma} & -\sigma & 1 \end{pmatrix} \begin{pmatrix} x \\ y \\ z \end{pmatrix}.$$

• $F_{1,v}^b$ is sent to $F_{2,v}^b$ and $F_{4,v}^b$ by rotations in \mathbb{R}^3 with an angle $\pm \frac{2\pi}{5}$ and an axis $\vec{u} := \frac{1}{\|\vec{OG}_3\|} \vec{OG}_3$, where G_3 denotes the center of $F_{3,v}^b$. We have: $\vec{u} = \frac{1}{\sqrt{5}\sqrt{2+\sigma}} (-\sqrt{5}\mathbf{j} + (\sigma+2)\mathbf{k})$. Once more we begin to calculate ρ a rotation in \mathbb{R}^3 with an angle $\frac{4\pi}{5}$ and an axis \vec{u} :

$$\begin{aligned} \rho \quad (x\mathbf{i} + y\mathbf{j} + z\mathbf{k}) &= \left[\frac{1}{2\sigma} \mathbf{1} + \frac{\sqrt{2+\sigma}}{2} \frac{1}{\sqrt{5}\sqrt{2+\sigma}} (-\sqrt{5}\mathbf{j} + (\sigma+2)\mathbf{k}) \right] [x\mathbf{i} + y\mathbf{j} + z\mathbf{k}] \left[\frac{1}{2\sigma} \mathbf{1} - \frac{\sqrt{2+\sigma}}{2} \frac{1}{\sqrt{5}\sqrt{2+\sigma}} (-\sqrt{5}\mathbf{j} + (\sigma+2)\mathbf{k}) \right]. \end{aligned}$$

So

$$\rho(x, y, z) = \frac{1}{2} \begin{pmatrix} -\sigma & -1 & -\frac{1}{\sigma} \\ 1 & -\frac{1}{\sigma} & -\sigma \\ \frac{1}{\sigma} & -\sigma & 1 \end{pmatrix} \begin{pmatrix} x \\ y \\ z \end{pmatrix}.$$

Hence $\rho^2 : F_{1,v}^b \rightarrow F_{2,v}^b$, and $\rho^3 : F_{1,v}^b \rightarrow F_{4,v}^b$. We have:

$$\rho^2(x, y, z) = \frac{1}{2} \begin{pmatrix} \frac{1}{\sigma} & \sigma & 1 \\ -\sigma & 1 & -\frac{1}{\sigma} \\ -1 & -\frac{1}{\sigma} & \sigma \end{pmatrix} \begin{pmatrix} x \\ y \\ z \end{pmatrix}, \quad \rho^3(x, y, z) = \frac{1}{2} \begin{pmatrix} \frac{1}{\sigma} & -\sigma & -1 \\ \sigma & 1 & -\frac{1}{\sigma} \\ 1 & -\frac{1}{\sigma} & \sigma \end{pmatrix} \begin{pmatrix} x \\ y \\ z \end{pmatrix}.$$

• $F_{1,v}^b$ is sent to $F_{5,v}^b$ by a rotation in \mathbb{R}^3 with an angle $\pm \frac{2\pi}{5}$ and an axis $\vec{u} := \frac{1}{\|\vec{OG}_6\|} \vec{OG}_6$, where G_6 denotes the center of $F_{6,v}^b$. We have: $\vec{u} = \frac{1}{\sqrt{5}\sqrt{2+\sigma}} (-(\sigma+2)\mathbf{i} - \sqrt{5}\mathbf{k})$. Once more we begin to calculate ρ a rotation in \mathbb{R}^3 with an angle $\frac{4\pi}{5}$ and an axis \vec{u} :

$$\begin{aligned} \rho \quad (x\mathbf{i} + y\mathbf{j} + z\mathbf{k}) &= \left[\frac{1}{2\sigma} \mathbf{1} + \frac{\sqrt{2+\sigma}}{2} \frac{1}{\sqrt{5}\sqrt{2+\sigma}} (-(2+\sigma)\mathbf{i} - \sqrt{5}\mathbf{k}) \right] [x\mathbf{i} + y\mathbf{j} + z\mathbf{k}] \left[\frac{1}{2\sigma} \mathbf{1} - \frac{\sqrt{2+\sigma}}{2} \frac{1}{\sqrt{5}\sqrt{2+\sigma}} (-(2+\sigma)\mathbf{i} - \sqrt{5}\mathbf{k}) \right]. \end{aligned}$$

So

$$\rho(x, y, z) = \frac{1}{2} \begin{pmatrix} 1 & \frac{1}{\sigma} & \sigma \\ -\frac{1}{\sigma} & -\sigma & 1 \\ \sigma & -1 & -\frac{1}{\sigma} \end{pmatrix} \begin{pmatrix} x \\ y \\ z \end{pmatrix}.$$

Hence $\rho^2 : F_{1,v}^b \rightarrow F_{5,v}^b$. We have:

$$\rho^2(x, y, z) = \frac{1}{2} \begin{pmatrix} \sigma & -1 & \frac{1}{\sigma} \\ 1 & \frac{1}{\sigma} & -\sigma \\ \frac{1}{\sigma} & \sigma & 1 \end{pmatrix} \begin{pmatrix} x \\ y \\ z \end{pmatrix}.$$

REFERENCES

- [1] R. AURICH, S. LUSTIG, F. STEINER. CMB anisotropy of the Poincaré dodecahedron. Class. Quantum Grav., 22: 2061-2083, 2005.
- [2] Ag. BACHELOT-MOTET. Wave Computation on the Hyperbolic Double Doughnut. J. Comp. Math., 28-6: 790-806, 2010.
- [3] S. CAILLERIE, M. LACHÎÈZE-REY, J.-P. LUMINET, R. LEHOUCQ, A. RIAZUELO, J. WEEKS. A new analysis of the Poincaré dodecahedral space model. Astron. Astrophys., 476-2: 691-696, 2007.
- [4] R. COOLS, A. HAEGEMANS. Algorithm 824: CUBPACK: a package for automatic cubature; framework description. ACM Trans. Math. Software, 29 (3), 287-296, 2003.
- [5] N. J. CORNISH, D. N. SPERGEL, G. D. STARKMAN. Circles in the sky: finding topology with the microwave background radiation. Class. Quantum Grav., 15: 2657-2670, 1998.
- [6] H. S. M. COXETER. Regular Polytopes. 3rd edn (New York: Dover), 1973.
- [7] E. GAUSSMANN, R. LEHOUCQ, J.-P. LUMINET, J.-Ph. UZAN, J. WEEKS. Topological lensing in spherical spaces. Class. Quantum Grav., 18: 5155-5186, 2001.
- [8] F. HECHT, A. LE HYARIC, O. PIRONNEAU. <http://www.freefem.org/ff++/>.
- [9] A. IKEDA. On the spectrum of homogeneous spherical space forms. Kodai Math. J., 18: 57, 1995.
- [10] M. LACHÎÈZE-REY. Eigenmodes of dodecahedral space. Class. Quantum Grav., 21:2455-2464, 2004.
- [11] Eigenmodes of three-dimensional spherical spaces and their application to cosmology. R. LEHOUCQ, J. WEEKS, J.-Ph. UZAN, E. GAUSSMANN, J.-P. LUMINET. Class. Quantum Grav., 19:4683-4708, 2002.
- [12] J.-P. LUMINET. The shape and topology of the universe. arXiv:0802.2236 [astro-ph], 2008.
- [13] J.-P. LUMINET, B. F. ROUKEMA. Topology of the universe: theory and observation. Theoretical and Observational Cosmology, 541:117-156, 1999.
- [14] J.-P. LUMINET, J. WEEKS, A. RIAZUELO, R. LEHOUCQ, J.-Ph. UZAN. Dodecahedral space topology as an explanation for weak wide-angle temperature correlations in the cosmic microwave background. Letters to nature, 425, 593:595, 2003.
- [15] B. F. ROUKEMA, T. A. KAZIMIERCZAK. The size of the Universe according to the Poincaré dodecahedral space hypothesis. arXiv:1106.0727v2 [astro-ph.CO], 2011.
- [16] P. SCOTT. The geometries of 3-manifolds. Bull. London. Math. Soc., 15:401-487, 1983.
- [17] G.F.E. SENDEN. The Topology of the Universe. Thesis: Rijksuniversiteit, Groningen, 2010.
- [18] H. SI. TetGen Users Guide: A quality Tetrahedral Mesh Generator and Three-Dimensional Delaunay Triangulator. <http://wias-berlin.de/software/tetgen/>.
- [19] C. WEBER, H. SEIFERT. Die beiden Dodekaederräume. Math. Z., 37:237-253, 1933.
- [20] J. WEEKS. Reconstructing the global topology of the universe from the cosmic microwave background. Class. Quantum Grav., 15: 2599-2604, 1998.
- [21] J. WEEKS. The Poincaré dodecahedral space and the mystery of the missing fluctuations. Notices of the AMS, 51-6: 610-619, 2004.
- [22] J. A. WOLF. Spaces of Constant Curvature. 5th edn (Boston, MA: Publish or Perish), 1967.
- [23] C. L. BENNETT, D. LARSON, J. L. WEILAND, N. JAROSIK, G. HINSHAW, N. ODEGARD, K. M. SMITH, R. S. HILL, B. GOLD, M. HALPERN, E. KOMATSU, M. R. NOLTA, L. PAGE, D. N. SPERGEL, E. WOLLACK, J. DUNKLEY, A. KOGUT, M. LIMON, S. S. MEYER, G. S. TUCKER, E. L. WRIGHT. Nine-Year Wilkinson Microwave Anisotropy Probe (WMAP) Observations: Final Maps and Results. arXiv:1212.5225v2 [astro-ph.CO], 2013.

UNIVERSITÉ DE BORDEAUX, INSTITUT DE MATHÉMATIQUES, UMR CNRS 5251, F-33405 TALENCE CEDEX
E-mail address: agnes.bachelot@math.u-bordeaux1.fr